FROM HYPOTHALAMIC PEPTIDES TO THE REGULATION OF DOPAMINE IN THE NUCLEUS ACCUMBENS: THE INTRODUCTION OF THE PARAVENTRICULAR NUCLEUS OF THE THALAMUS IN A NOVEL HYPOTHALAMIC-THALAMIC-STRIATAL CIRCUIT

MATTHEW PARSONS

NOTE TO USERS

FROM HYPOTHALAMIC PEPTIDES TO THE REGULATION OF DOPAMINE IN THE NUCLEUS ACCUMBENS: THE INTRODUCTION OF THE PARAVENTRICULAR NUCLEUS OF THE THALAMUS IN A NOVEL HYPOTHALAMIC-THALAMIC-STRIATAL CIRCUIT

By

Matthew Parsons

A thesis submitted to the

School of Graduate Studies

in partial fulfillment of the

requirements for the degree of

Master of Science

Faculty of Medicine

Memorial University of Newfoundland

May 2006

St John's Newfoundland

Your file Votre référence
ISBN: 978-0-494-30497-6
Our file Notre référence
ISBN: 978-0-494-30497-6

Abstract

Previous studies have demonstrated that the paraventricular nucleus of the thalamus (PVT) receives heavy projections from numerous hypothalamic peptides involved in energy homeostasis and brainstem monoamines involved in various aspects of stress and arousal. Not surprisingly, the PVT is highly active during periods of active waking as well as stress and lesions of the PVT influence feeding behavior and anticipatory reactions to cues signaling food reward. Furthermore, the PVT sends a dense glutamatergic projection to the same regions of the nucleus accumbens shell (NacSh) receiving heavy dopaminergic innervation from the ventral tegmental area. Although numerous cortical afferents to the accumbens have been shown to mediate a glutamate-dependent regulation of dopamine efflux within the NacSh, little is known regarding the role of PVT terminals within this region of the ventral striatum. Initial anatomical experiments were done to examine the innervation of the PVT and adjacent thalamic nuclei by two recently discovered hypothalamic peptides termed the orexins and cocaine and amphetamine related transcript (CART), both of which have been heavily implicated in stress and arousal as well as energy homeostasis. Specifically, orexin and CART peptides fibers were investigated in terms of their relationship and proximity to PVT neurons projecting to the NacSh. Further experiments were done using *in vivo* voltammetry to examine the effects of electrical stimulation of the PVT on dopamine efflux in the NacSh. The PVT was found to receive heavy projections from both orexin immunopositive and

CART immunopositive fibers whereas adjacent thalamic nuclei received considerably less or no innervation whatsoever from either peptide. Orexin and CART fibers in the PVT were found to co-express immunoreactivity for synaptophysin, a marker for presynaptic exocytotic release, suggesting that these neuropeptides are actively released within the PVT. High magnification confocal and light microscopy revealed frequent appositions between orexin and CART fiber varicosities and PVT neurons projecting to the NacSh. Voltammetric recordings from the NacSh demonstrated that brief electrical stimulation of the PVT (400 μA, 40 Hz, 1.0 ms for 5s) resulted in a transient increase in dopamine oxidation current within the NacSh. The PVT-evoked response was found to be insensitive to inhibition of midbrain dopamine neurons, suggesting a presynaptic regulation of dopamine release. Indeed, an immediate attenuation of PVT evoked dopamine transients was observed upon intra-accumbens infusion of the ionotropic glutamate receptor antagonist kynurenic acid. It is hypothesized that this hypothalamic-thalamic-striatal circuit is important in the facilitation of specific motivated behaviors and is discussed in terms of both a stress and arousal induced increase in dopamine efflux as well as a dopaminergic modulation of food-seeking behavior.

Acknowledgements

I would like to thank Dr. Gilbert Kirouac, my supervisor, for providing me with the best possible guidance a student could ask for.

I would also like to thank Sa Li, for teaching me all the skills necessary to complete this thesis.

I would also like to thank Dr. Michiru Hirwasawa, my co-supervisor, for all her advice and support throughout my master's training.

I would also like to thank my supervisory committee members, Drs. John McLean and Dale Corbett, as well as the rest of the faculty and staff within the faculty of medicine.

Finally, I would like to thank NSERC for providing the funding for my master's training.

Table of Contents

List of Figures

Chapter 1

Introduction

1.1 The midline and intralaminar thalamus

The midline and intralaminar thalamus was introduced as a group of diencephalic nuclei that collectively formed part of an ascending reticular activating system contributing to general cortical arousal (Groenewegen & Berendse, 1994; Van der Werf *et al.*, 2002). An extensive relay role for these thalamic nuclei was suggested by early tract tracing studies revealing widespread cortical afferents originating from neurons throughout the midline and intralaminar thalamus (Royce *et al.*, 1989). However, recent investigations using more sensitive tract tracing techniques have demonstrated that the individual thalamic nuclei within this complex project to distinct cortical and subcortical forebrain areas (Bubser & Deutch, 1998; Moga *et al.*, 1995; Su & Bentivoglio, 1990; Van der Werf *et al.*, 2002). Research has since been directed at anatomically and functionally defining each individual nucleus within the midline and intralaminar thalamus. A recent review (Van der Werf *et al.*, 2002) separates the midline and intralaminar nuclei into four groups based on their efferent projection patterns (Fig 1.). First, the awareness of viscerosensory stimuli is attributed to a dorsal group that includes the paraventricular, paratenial, and intermediodorsal nuclei and their projections to the ventral striatum,

Fig. 1. Schematic diagram highlighting the locations and projections of three of the four "groups" of midline and intralaminar nuclei as proposed by Van der Werf (2000). Numbers indicate approximate distance from bregma. 3V, third ventricle; ACM, anterior central medial nucleus; CL, central lateral nucleus; fr, fasciculus retroflexus; IMD, Intermediodorsal nucleus; PC, paracentral nucleus; PCM, posterior central medial nucleus; PT, paratenial nucleus; Re, nucleus reunions; Rh, rhomboid nucleus; sm, stria medullaris.

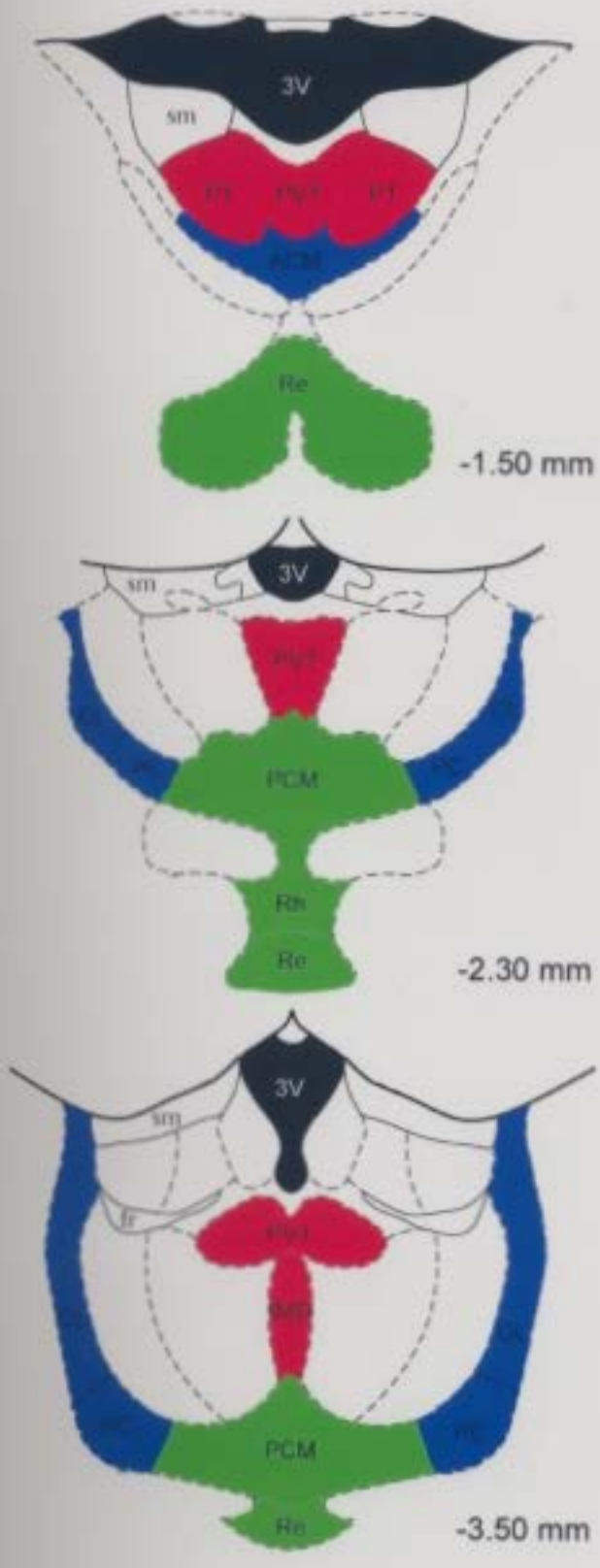

Dorsal Group projects to:
-Ventral Striatum
-Amygdala
-Pre- and Infralimbic Cortex

Lateral Group projects to:
-Dorsal Prefrontal Cortex
-Dorsal Striatum
-Cingulate Cortex

Ventral Group projects to:
-Hippocampus
-Primary Motor Cortex
-Primary Sensory Cortex
-Association Cortical Areas

* Posterior Group (not shown) projects to:
-Caudate and Putamen
-Globus Pallidus
-Substantia Nigra
-Subthalamic Nucleus

amygdala, and the pre- and infralimbic cortices. Second, a lateral group that includes the paracentral, central lateral and anterior central medial nuclei, plays a role in cognitive awareness via projections to the dorsal striatum and cingulate cortex. Third, the reuniens, rhomboid and posterior central medial nuclei make up a ventral group that projects to non-limbic cortical regions and is involved in polymodal sensory awareness. Last, a posterior group involved in the generation of motor responses to stimulus awareness includes the centre median and parafascicular nuclei and projections to the sensory and motor cortices. An overview of these thalamic groups can be seen in Figure 1. Of interest to the present experiments is the dorsal group, in particular, the paraventricular nucleus of the thalamus (PVT) and its heavy glutamatergic projection to the shell of the nucleus accumbens (NacSh).

1.2 The Paraventricular Nucleus of the Thalamus (PVT)

1.2.1 Afferents of the PVT

The PVT is a small nucleus within the midline and intralaminar complex. Located on the midline immediately ventral to the third ventricle, the PVT is thought to contribute to forebrain arousal and awareness by receiving a wide array of arousal-related information from the brainstem and hypothalamus (Groenewegen & Berendse, 1994; Van der Werf *et al.*, 2002). The PVT receives projections from nociceptive and visceral relays in the brainstem including the periaqueductal grey, parabrachial and solitary tract nuclei (Chen & Su, 1990; Cornwall & Phillipson, 1988; Krout *et al.*, 2002; Krout & Loewy, 2000a, 2000b; Ruggiero *et al.*, 1998). Hypothalamic areas involved in stress and arousal as well as homeostatic and circadian regulation also heavily innervate the PVT (Cornwall & Phillipson, 1988; Kirouac *et al.*, 2005; Novak *et al.*, 2000a; Otake, 2005; Otake & Ruggiero, 1995; Parsons *et al.*, 2006). In general, the innervation patterns found within the PVT are unique compared to other midline and intralaminar nuclei. For example, the PVT can be distinguished from adjacent nuclei based on a dense innervation by norepinephrine fibers originating in the locus coeruleus (B. E. Jones & Yang, 1985) and serotonin fibers likely originating from the dorsal and median raphe (Freedman & Cassell, 1994; Krout *et al.*, 2002). Arousal and feeding related peptides such as alpha melanocortin stimulating hormone (MSH) and neuropeptide Y also heavily innervate the PVT while largely avoiding adjacent nuclei (Freedman & Cassell, 1994). The unique

innervation patterns within the PVT place this nucleus in an anatomical position to integrate the net activity of numerous hypothalamic peptides and brainstem monoamines.

1.2.2 Efferents of the PVT

Similar to PVT afferents, the efferent projections of the PVT are quite unique in comparison to adjacent thalamic nuclei. Within the entire midline and intralaminar thalamic complex, the PVT is the only nucleus to send a dense projection to the nucleus accumbens (Berendse & Groenewegen, 1990; Bubser & Deutch, 1998; Hagan *et al.*, 1999; Moga *et al.*, 1995; Pinto *et al.*, 2003; Su & Bentivoglio, 1990; Van der Werf *et al.*, 2002). Other projections from the PVT have been observed to terminate within regions of the hypothalamus, hippocampus, amygdala and prefrontal cortex (Moga *et al.*, 1995; Su & Bentivoglio, 1990; Van der Werf *et al.*, 2002). More specifically, the PVT projects to the suprachiasmatic, dorsomedial and lateral hypothalamic nuclei. Projections to the amygdala preferentially target the central, basomedial and basolateral nuclei while hippocampal projections specifically target the ventral subiculum. Innervation of the prefrontal cortex includes the deep layers of the prelimbic and infralimbic cortex while fibers coursing towards the striatum terminate with the highest density in the shell of the nucleus accumbens (NacSh), a region implicated in motivated behavioral responding. Anatomically, it can be proposed that the PVT integrates the net activity of numerous arousal-related afferents and relays this information to the NacSh in order to influence behavioral patterns.

1.2.3 Functional implications of the PVT

As mentioned in section 1.2.1, the PVT receives visceral sensory information from the parabrachial and solitary tract nuclei within the brainstem and projects to the infralimbic cortex that is involved in visceral motor functions (Berendse & Groenewegen, 1991; Chen & Su, 1990; Cornwall & Phillipson, 1988; Krout *et al.*, 2002; Krout & Loewy, 2000a, 2000b; Moga *et al.*, 1995; Ruggiero *et al.*, 1998). This anatomical connectivity has lead researchers to believe that the PVT functions in part to relay visceral sensory information to the cortex (Otake & Nakamura, 1998; Van der Werf *et al.*, 2002). However, if one considers the overall anatomical properties of the PVT, especially the observation that the heaviest efferents of the PVT target the NacSh, it is likely that the PVT is involved in behavioral state changes induced by general stress and arousal, in which visceral arousal and nociception are included. Studies using c-fos mRNA or Fos protein expression to represent neuronal activity show that the PVT is consistently active across numerous stress paradigms and during periods of active waking and arousal (Bhatnagar & Dallman, 1998; Bubser & Deutch, 1999; Novak & Nunez, 1998; Novak *et al.*, 2000b; Otake *et al.*, 2002; Peng *et al.*, 1995). In addition, heavy innervation of the PVT by feeding-related peptides such as neuropeptide Y and alpha-MSH (Freedman & Cassell, 1994) suggest that information reflecting the hunger state of an animal may also alert the forebrain through a PVT relay. In support of this, food deprivation or restriction increases the activity of PVT neurons (Nakahara *et al.*, 2004). Two novel peptides implicated in arousal and energy homeostasis, termed the orexins and

cocaine and amphetamine related transcript (CART), project throughout the brain and may contribute to an arousal-induced activation of PVT neurons.

1.3 Novel Neuropeptides projecting to the PVT

1.3.1 The orexins

The orexin (hypocretin) neuropeptides were discovered in 1998 (de Lecea *et al.*, 1998; Sakurai *et al.*, 1998) and have become a topic of major interest in research concerning sleep-wake regulation as well as stress and arousal. The active orexin-A (hypocretin-1) and orexin-B (hypocretin-2) peptides are formed from proteolytic cleavage of the 130 amino acid precursor prepro-orexin (prepro-hypocretin). The orexins bind to two similar G-protein coupled receptors termed orexin receptor 1 (OX1R) and orexin receptor 2 (de Lecea *et al.*, 1998; Sakurai *et al.*, 1998). Orexin-A and orexin-B are co-localized within neurons of the lateral hypothalamus and innervate widespread regions of the CNS including the hypothalamus, midline thalamus, cortex, septal area, amygdala, and many brainstem areas including monoaminergic and cholinergic cell groups (Cutler *et al.*, 1999; Date *et al.*, 1999; Nambu *et al.*, 1999; Peyron *et al.*, 1998). In line with their widespread projections, numerous behavioral and physiological functions have been ascribed to orexins including stimulation of wakefulness, feeding and locomotor activity, as well as regulation of the autonomic and neuroendocrine systems (Beuckmann & Yanagisawa, 2002; de Lecea *et al.*, 2002; Ferguson & Samson, 2003; Kukkonen *et al.*,

2002; Rodgers *et al.*, 2002; Siegel, 2004; Taheri *et al.*, 2002; Willie *et al.*, 2001). Functional differences between the two orexin peptides are unclear and, because they are co-localized within the same neurons, the term "orexins" will be used throughout to refer to both orexin-A and orexin-B.

1.3.2 Cocaine and amphetamine related transcript (CART) peptide

A fragment of the CART peptide was first reported in 1981 (Spiess *et al.*, 1981) and it was discovered years later that the mRNA encoding this peptide fragment was increased following administration of either cocaine or amphetamine (Douglass *et al.*, 1995). Unlike the orexins, CART peptide is produced in multiple regions throughout the brain including the nucleus accumbens, lateral hypothalamus, and the arcuate, solitary tract and parabrachial nuclei (Koylu *et al.*, 1998; Koylu *et al.*, 1997). CART-containing fibers project to widespread areas of the brain including the midline thalamus and a majority of other regions innervated by the orexin peptide fibers (see section 1.3.1). Since its discovery, CART has been implicated in numerous physiological processes including the regulation of food intake, reward and reinforcement, as well as stress and arousal (Dominguez *et al.*, 2004; Hunter *et al.*, 2004).

1.3.3 Functional implications of orexin and CART innervation of the PVT

Behavioral and *in situ* hybridization data reveal a role for both the orexin and CART peptides in the control of food intake. Central administration of orexins can promote food intake (Dube *et al.*, 1999; Ramsey *et al.*, 2005; Sakurai *et al.*, 1998; Sweet *et al.*, 1999) and fasting up-regulates orexin mRNA (X. J. Cai *et al.*, 1999; Sakurai *et al.*, 1998). Conversely, central administration of CART peptide inhibits food intake (Lambert *et al.*, 1998; Rohner-Jeanrenaud *et al.*, 2002; Tachibana *et al.*, 2003; Vrang *et al.*, 1999) and fasting decreases CART mRNA in the hypothalamus (Kristensen *et al.*, 1998; Li *et al.*, 2002; Savontaus *et al.*, 2002). The connection between these peptides and energy homoeostasis is consistent with a potential role of the PVT in food intake. Lesions of the PVT have been reported to influence feeding behavior (Bhatnagar & Dallman, 1999) and to attenuate the increases in both locomotor activity and blood-corticosterone levels normally seen during the anticipation of food reward (Nakahara *et al.*, 2004). The orexin and CART peptides may contribute to food seeking behaviors in part through a PVT relay to the forebrain.

Another major role for the orexins is in the maintenance of general arousal and regulation of the sleep-wake cycle. This is evident in animals with disruptions in aspects of the orexin system. For example, mutation of prepro-orexin or the OX2R gene (knockout mice), genetic ablation of orexin neurons (orexin/ataxin-3 transgenic mice) and lesions of orexin neurons with the ribosome-inactivating protein saporin toxin in adult rats produce animals with disrupted patterns of wakefulness and phenotypes

resembling human narcolepsy (Beuckmann *et al.*, 2004; Chemelli *et al.*, 1999; Gerashchenko *et al.*, 2001; Hara *et al.*, 2001; Willie *et al.*, 2003). Consistent with these experimental studies, postmortem analyses of brains from dogs or humans with narcolepsy show abnormalities in the orexin system (Nishino *et al.*, 2001; Nishino *et al.*, 2000; Thannickal *et al.*, 2000) and suggests that the orexins are necessary for the maintenance of wakefulness. This is consistent with studies demonstrating increased orexin activity during periods of active waking, high arousal or stress (Espana *et al.*, 2003; Kodama *et al.*, 2005; Yoshida *et al.*, 2001). It has recently been shown that orexin neurons projecting to the PVT are randomly distributed throughout the orexin neuron population (Kirouac *et al.*, 2005) which suggests that the PVT is influenced by the activity of the orexin population as a whole and supports the idea that the PVT receives a wide array of general arousal information.

It has been reported that adrenalectomy decreases CART mRNA and peptide levels in hypothalamic regions and that this decrease is alleviated by corticosterone administration (Balkan *et al.*, 2003; Balkan *et al.*, 2001; Savontaus *et al.*, 2002; Vrang *et al.*, 2003). These data suggest that arousal and stress can regulate CART synthesis and expression. The CART-producing neurons most associated with the stress response, as defined by the effect of adrenalectomy on CART mRNA and peptide levels, are found in the arcuate nucleus of the hypothalamus (Dominguez *et al.*, 2004). Interestingly, it has recently been shown that the majority of CART innervation of the PVT arises from neurons in the arcuate nucleus (Kirouac *et al.*, in press) and suggests that the CART projection to the PVT is important in the relay of stress-related information. Overall, the

PVT receives a wide range of afferent information: hunger and satiety signals from hypothalamic peptides; stress and arousal signals from hypothalamic peptides and brainstem monoamines; and visceral sensory and nociceptive signals from various brainstem relay nuclei. In light of this, the PVT is likely a region where an overall level of general arousal is integrated before being sent to the shell of the nucleus accumbens.

1.4 The nucleus accumbens shell

1.4.1 The nucleus accumbens can be divided into core and shell subregions

The ventral striatum refers to a collection of brain regions in the forebrain which receive afferent input from limbic structures such as the medial prefrontal cortex, amygdala and hippocampus as well as the PVT of the midline thalamus. The ventral striatum has been referred to as the limbic-motor interface based in part on the limbic input it receives and its heavy efferent projections to the ventral pallidum, a structure closely tied to motor output systems (for review see Mogenson *et al.*, 1980). The most prominent region of the ventral striatum is the nucleus accumbens. The nucleus accumbens itself can be divided into two subregions that have been termed the "core" and "shell" of the nucleus accumbens. Interest in the nucleus accumbens began with early reports (Matthysse, 1973; Stevens, 1973) linking the mesolimbic dopamine system, which includes a dense dopamine projection from the midline ventral tegmental area (VTA) to the nucleus accumbens, to schizophrenic symptoms. Since then the accumbens

has been shown to play a key role in substance abuse as well as normal reward-related and motivated behaviors (for review see Heimer *et al.*, 1997; Mogenson *et al.*, 1980; Mogenson and Yang, 1991; Salamone *et al.*, 2005. Included in the nucleus accumbens is a central core which is surrounded medially, ventrally and laterally by the shell region. The two divisions are commonly distinguished by immunoreactivity against the calcium binding protein calbindin (Zahm, 1992), with immunoreactivity being weak in the shell and dense in the core.

Both regions of the nucleus accumbens are heterogeneous in terms of its afferent and chemical composition. Thoroughly summarized by Heimer *et al.*, (1997), the core contains "patches" of tissue where immunoreactivity for the opioid peptide enkephalin is dense and dopamine immunoreactivity is weak. The PVT and lateral prefrontal cortex project to these areas of the nucleus accumbens core. Conversely, adjacent regions of the core exhibiting strong dopamine and weak enkephalin immunoreactivity receive afferents from the basolateral amygdala and prelimbic cortex. The shell of the nucleus accumbens contains cell-dense regions characterized by low enkephalin and dopamine immunoreactivity. Interestingly, areas of low cell density within the shell receive dense dopamine innervation from the VTA and heavy glutamate afferents from the ventral subiculum and the PVT. This anatomical heterogeneity may have a functional role, and suggests an importance of glutamatergic PVT projections to dopamine-rich areas of the NacSh.

Zahm (2000) has placed the subdivisions of the nucleus accumbens into separate "networks" based largely on efferent connectivity. The shell network projects to regions

such as the ventromedial ventral pallidum, preoptic area, lateral hypothalamus, VTA and periaqueductal grey, which the author refers to as more "limbic-like" regions associated with motivated and goal-directed behaviors. The core network includes the dorsolateral ventral pallidum, entopeduncular nucleus, subthalamic nucleus and substantia nigra, which the author refers to as more "basal ganglia-like" regions associated with motor output. This is fitting with the nucleus accumbens as the "limbic-motor interface" participating in converting motivation to action, with the shell region concerned more with integrating the activity of numerous limbic inputs and the core region concerned with sending appropriate signals to motor output systems.

1.4.2 Dopamine in the NacSh: Gating cortical inputs

Dopamine release in the NacSh has typically been referred to as the "natural reinforcement system" thought to directly mediate the rewarding properties of natural reinforcers and drugs of abuse. However, it has become clear that dopamine is involved in several aspects of associative learning including aversive learning and therefore cannot be responsible for euphoric feelings upon receipt of a natural reward or drug of abuse (Blackburn *et al.*, 1992; Salamone *et al.*, 2003). It is now widely accepted that dopamine release within the NacSh from VTA terminals plays a critical role in the selection and facilitation of motivated behavioral responses. As mentioned, numerous glutamate afferents overlap within dopamine-rich regions of the NacSh. Specifically, the NacSh received goal-oriented cognitive information from the prefrontal cortex, affective

information from the amygdala, and contextual information from the hippocampus (Grace, 2000). The NacSh is thought to play a role in motivation by acting as a "gate" or "filter" having the ability to strengthen or weaken the relative effectiveness each of these glutamatergic afferents have on behavioral output (Grace, 2000; Salamone *et al.*, 2005). For example, prefrontal cortex stimulation excites medium spiny output neurons of the NacSh but this excitation is attenuated by agonist actions at D2 receptors presumably located on corticoaccumbens terminals (Grace, 2000). Furthermore, bath application of dopamine attenuates medium spiny neuron excitation evoked by stimulation of the amygdala or hippocampus and this attenuation is blocked upon administration of D1 receptor antagonists (Charara & Grace, 2003). Thus, dopamine is hypothesized to influence motivated or goal directed behaviors through an ability to modulate the effect of limbic cortical afferents on the excitability of medium spiny output neurons.

1.4.3 The regulation of dopamine release in the NacSh

It has been proposed (Grace, 1991) that glutamate release in the nucleus accumbens can act locally on dopamine terminals to modulate the levels of sustained tonic (extrasynaptic) dopamine. This theory states that tonic levels of dopamine set a background level of receptor activation that potentiates the effects of phasic dopamine release initiated by the burst firing of dopamine neurons. Although the exact role of dopamine in the NacSh is complex and yet to be fully understood, the necessity for a tight regulation of dopamine is evident in psychiatric disorders such as schizophrenia,

attention deficit hyperactivity disorder, and drug abuse, which are all linked to a dysregulation of the dopamine system.

The PVT sends a moderate glutamate projection to the core of the nucleus accumbens and a dense glutamate projection to the NacSh (Groenewegen & Berendse, 1994; Moga *et al.*, 1995; Pinto *et al.*, 2003; Van der Werf *et al.*, 2002). The regions of the NacSh innervated by the PVT also exhibit dense immunoreactivity for tyrosine hydroxylase, which is likely to represent axon terminals from dopamine neurons in the VTA (Pinto *et al.*, 2003). Although no axo-axonic synapses between glutamate and dopamine terminals in the NacSh have been observed to date, numerous studies suggest that exogenous glutamate application or endogenous glutamate release can act locally within the NacSh to regulate dopamine release (Borland & Michael, 2004; David *et al.*, 2005; Kulagina *et al.*, 2001; Morari *et al.*, 1998; Whitton, 1997). The PVT, through receiving numerous arousal related afferents, may be involved in arousal-induced maintenance of dopamine tone within the NacSh.

1.4.4 Dopamine, stress and food intake

Various techniques that quantify the concentration of dopamine within a brain region over time have all consistently shown that dopamine levels within the NacSh are increased following exposure to an acute stressor. By measuring the DOPAC:DA ratio in the NacSh, it was demonstrated that acute immobilization stress increases dopamine utilization in the shell but not core of the nucleus accumbens (Deutch & Cameron, 1992).

Similarly, application of mild footshock to rats increased the dopamine concentration in a microdialysis sample taken from the NacSh (Kalivas & Duffy, 1995). Voltammetric recordings also confirm stress induced dopamine release within the NacSh by showing an increase in dopamine oxidation current within the NacSh following tail pinch and restraint stress (D'Angio *et al.*, 1987; Doherty & Gratton, 1992). However, repeated exposure to unavoidable stressors decreases an animal's behavioral response to subsequent acute stressors and this behavioral depression is associated with a decrease in dopamine levels within the NacSh (Gambarana *et al.*, 1999) that may be mediated by glutamatergic afferents.

The functional role of dopamine levels in the NacSh is certainly not exclusive to stress and arousal, as it is well known that a complex relationship exists between dopamine and feeding. Increases in NacSh dopamine levels are associated with both food seeking and consummatory behaviors, although various arguments have been made supporting a dopaminergic involvement solely in the initiation and maintenance of foraging behavior rather than actual consummation of a food. Infusions of dopamine directly into the NacSh elicits a feeding response (Swanson *et al.*, 1997) and blockade of the D1 receptor attenuates the increase in feeding induced by an intra-accumbens infusion of μ-opioid receptor agonists (Ragnauth *et al.*, 2000). Additionally, recording dopamine levels in the NacSh of behaving animals reveals that increased dopamine efflux can be seen upon anticipation of a predicted food reward (Roitman *et al.*, 2004) as well as during intake of palatable foods (Bassareo & Di Chiara, 1999). Interestingly, infusion of glutamate agonists and antagonists into the NacSh profoundly influences the feeding

response (Maldonado-Irizarry *et al.*, 1995), and may reflect the effects of a glutamatergic presynaptic regulation of striatal dopamine release.

1.5 Glutamatergic regulation of dopamine

1.5.1 Glutamate regulation of dopamine: *In vitro* studies

The effects of intra-striatal infusion of glutamate agonists and antagonists on dopamine levels in the dorsal striatum and nucleus accumbens have produced mixed findings. While controversial, there is substantial evidence showing that application of glutamate agonists and antagonists in the nucleus accumbens can locally increase and decrease dopamine levels, respectively (Borland & Michael, 2004; David *et al.*, 2005; Kulagina *et al.*, 2001; Morari *et al.*, 1998; Whitton, 1997). Application of NMDA in the absence of Mg++ was found to increase dopamine release in rat striatal synaptosomes and this effect was blocked by either Mg++ or selective NMDA receptor antagonists (Johnson & Jeng, 1991; Krebs *et al.*, 1991; Wang, 1991). The same authors further demonstrated that application of AMPA and kainate in the presence of Mg++ increases dopamine release from rat striatal synaptosomes and is blocked using selective non-NMDA receptor antagonists. Studies done in rat striatal slices have shown similar results in that NMDA applied in Mg++ free conditions dose-dependently increases dopamine release from striatal slices (N. S. Cai *et al.*, 1991; Clow & Jhamandas, 1989; Krebs *et al.*, 1991). Furthermore, application of L-glutamate in Mg++ free conditions induces an

NMDA receptor dependent dopamine efflux in the striatal slice (Bowyer *et al.*, 1991). However, in the presence of Mg++, L-glutamate evokes a response of a smaller magnitude, confirming that glutamate actions at non-NMDA receptors also have a stimulatory effect on dopamine release. The tendency for local ionotropic glutamate agonists to increase striatal dopamine efflux occurs at least in part by an impulse independent mechanism as intra-VTA infusions of tetrodotoxin, a substance commonly used to prevent action potential firing, fails to block the dopamine response (Iravani & Kruk, 1996; Krebs *et al.*, 1991). Interestingly, one study has shown that electrically evoked dopamine release is facilitated by AMPA/kainate receptor activation in the absence of Mg++ and by NMDA receptor activation in Mg++-free conditions (Antonelli *et al.*, 1997). Together these data suggest that ionotropic glutamate receptors have a tendency to influence both impulse dependent and impulse independent dopamine release.

1.5.2 Glutamate regulation of dopamine: *In vivo* studies

The NacSh receives glutamate afferents from numerous sources including the PVT, hippocampus, amygdala, and prefrontal cortex. *In vivo* data show that electrical stimulation of the ventral subiculum of the hippocampus and the basolateral nucleus of the amygdala results in impulse independent dopamine efflux in the nucleus accumbens (Blaha *et al.*, 1997; Floresco *et al.*, 1998; Howland *et al.*, 2002). The evoked response appeared to be mediated by glutamate receptors in the nucleus accumbens because local

applications of ionotropic receptor blocking agents attenuated the response whereas inactivation of dopamine neurons in the VTA had no effect. This suggests that limbic areas sending a glutamate projection to the nucleus accumbens may facilitate impulse independent dopamine release and influence tonic dopamine tone in this area of the striatum. The data obtained from both *in vitro* and *in vivo* studies collectively suggest that glutamate actions at ionotropic receptors in the striatum can evoke local impulse independent dopamine release.

1.5 Summary and Hypothesis

The PVT can be separated from adjacent midline and intralaminar thalamic nuclei based on efferent projections to limbic forebrain regions, with an especially dense innervation of the NacSh. Furthermore, afferents to the PVT include a wide variety of brainstem monoamines and hypothalamic peptides involved in many aspects of stress, food intake and general arousal. The experiments in this thesis can be divided into two sections with the first designed to describe the PVT innervation by the novel orexin and CART peptides. Orexin containing cell bodies are found within the lateral hypothalamus and perifornical area while neurons immunoreactive for the CART peptide are dispersed throughout numerous regions of the hypothalamus and brainstem. Although orexin and CART fibers have been previously shown to innervate the PVT, the anatomical data in the present thesis provides a full description of orexin and CART immunoreactivity throughout the entire midline and intralaminar thalamus as well as the proximity of these

fibers to PVT neurons projecting to the NacSh. The PVT projection to the nucleus accumbens preferentially targets dopamine-rich striatal tissue while avoiding areas of weak dopamine activity. Numerous *in vivo* and *in vitro* studies suggest that glutamatergic afferents to the striatum, including the NacSh, can regulate local dopamine release by acting presynaptically at dopamine terminals. The release of dopamine in the NacSh is thought to facilitate behavioral activity and play a role in the expression of motivated behaviors. The second section of this thesis is designed to investigate, using *in vivo* voltammetry, any potential modulation of NacSh dopamine levels by glutamate projections from the PVT to the NacSh. I hypothesize that orexin and CART fibers in the PVT appose PVT neurons projecting to the NacSh. Furthermore, it is expected that excitation of PVT neurons results in an increase in tonic dopamine levels in the NacSh. Such information may introduce the PVT as a critical cell group involved in processing an overall level of arousal information and communicating this to the NacSh where it can influence tonic dopamine levels and thereby modify the expression of motivated behaviors. This proposal is presented as a schematic in Figure 2.

Fig. 2. Schematic diagram highlighting anatomical properties of the paraventricular nucleus of the thalamus (PVT). The PVT likely plays a role in the integration and relay of arousal-related information to the nucleus accumbens shell (NacSh) where it may act to increase dopamine (DA) release and influence behavioral output. Numerous neurotransmitters are released in the PVT including the orexins, CART, norepinephrine, serotonin, neuropeptide Y (NPY), alpha-melanocortin stimulating hormone (MSH), and corticotrophin releasing factor (CRF). The majority of PVT innervation originates from neurons in various brainstem and hypothalamic nuclei.

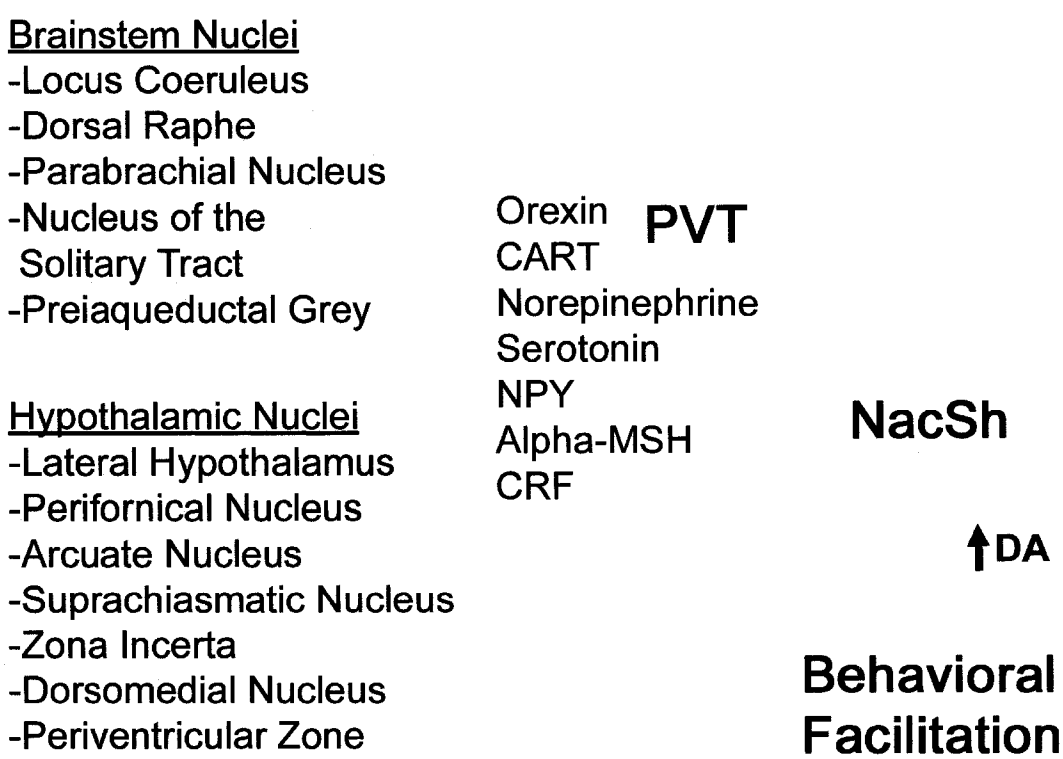
Brainstem Nuclei
-Locus Coeruleus
-Dorsal Raphe
-Parabrachial Nucleus
-Nucleus of the
Solitary Tract
-Preiaqueductal Grey
Hypothalamic Nuclei
-Lateral Hypothalamus
-Perifornical Nucleus
-Arcuate Nucleus
-Suprachiasmatic Nucleus
-Zona Incerta
-Dorsomedial Nucleus
-Periventricular Zone
Orexin
CART
Norepinephrine
Serotonin
NPY
Alpha-MSH
CRF
PVT
NacSh
DA
Behavioral
Facilitation

2.2 Orexin and CART innervation of PVT neurons projecting to the NacSh

2.2.1 Iontophoresis

Cholera toxin b (CTb; List Biological Laboratory, Campbell, CA) and fluorogold (FG; Molecular Probes) were used for the retrograde tract tracing experiments. Subjects were anesthetized with equithesin (0.3ml/100g, i.p.), placed in a Kopf stereotaxic frame, and a hand drill was used to expose the brain surface above the striatum. The dura was removed at the exposed site and a glass pipette (5-10 μm O.D.) filled with retrograde tracer solution was positioned 2.0 mm anterior and 1.2 mm lateral to bregma then lowered 6.5 mm ventral to the brain's surface. Either 0.5% CTb or 1.0% FG (CTb dissolved in physiological saline, FG in 0.1M cacodylate buffer) was injected iontophoretically by application of a 3 to 5 μA positive current (200 msec pulses at 2 Hz for 15 minutes). Pipettes were left in place for an additional 2 minutes following iontophoresis before removal from the brain. The incision was sutured and subjects were allowed 7-14 days to recover. A total of 10 animals (6 FG and 4 CTb) were used in the retrograde tracing experiments.

In an attempt to completely fill the soma and dendrites of PVT neurons, neurobiotin was iontophoretically applied to various anteroposterior levels of the PVT. Pipettes (5-10 μm O.D) were filled with 1.5% neurobiotin (Vector Laboratories) in 0.5 M NaCl, and a 3-5 μA positive current (500 ms pulses at 10 Hz for 15 minutes) was applied.

Three rats were used and each animal received 2-4 different injections made at various co-ordinates within the dorsal thalamus (0.8 mm lateral, 5.0 mm ventral, and -3.3, -3.0, -2.7, -2.4 mm posterior; angled 10° in the medial-lateral plane). Animals were given 1-3 days to recover.

2.2.2 Tissue preparation

All animals were perfused through the ascending aorta with 150-200 ml of warm heparinized saline followed by 450-500 ml of ice cold 4% paraformaldehyde. Brains were removed, post-fixed in the same fixative for 2-4 hours, and then immersed in graded sucrose concentrations over two days (10 and 20% w/v). Tissue was frozen quickly using Fisherbrand Histo-freeze and coronal sections of the brain were cut at 50 μm on a cryostat.

The nature of the study demanded the use of multiple immunochemical combinations to avoid host species overlap of the primary antibodies. All tissue was pre-incubated in blocking solution (5% normal donkey serum, 0.3% triton X-100, 0.1% sodium azide) for one hour at room temperature prior to primary antibody incubation. With the exception of the injection sites, all tissue was incubated in the appropriate primary antibody cocktail for 24 hours at room temperature and another 24 hours at 4°C. All fluorophore-conjugated secondary antibody incubations were done for 2-4 hours at room temperature. All antibodies were diluted in the blocking serum and tissue was rinsed thoroughly in PBS between each immunochemical step. Following each

immunochemical protocol, sections were rinsed and mounted onto gelatin-coated slides where they were left overnight to dry. Slides were then immersed in a series of graded alcohol concentrations, cleared in xylene, and coverslipped.

2.2.3 Immunohistochemistry

2.2.3.1 Confirmation of injection sites

Sections of the nucleus accumbens were incubated overnight at room temperature in either goat anti-CTb (1:40,000; List Biological, catalogue #703, lot #7032H) or rabbit anti-FG (1:40,000; Chemicon, catalogue #AB153, lot #24110032), depending upon which tracer injection the animal received. Tissue from animals receiving CTb injections was then incubated in a biotinylated donkey anti-goat secondary antibody (1:500; Jackson Immunoresearch) for 2-4 hours at room temperature, then for 2 hours in an avidin biotin complex prepared according to kit direction (Elite ABC Kit, Vector Laboratories, Burlingame, CA). The histochemical product was visualized by brief exposure to 2,4 diaminobenzidine (DAB; DAB Kit, Vector Laboratories), prepared according to kit directions. Similar steps were used for those animals receiving rabbit anti-FG injections except the secondary antibody used was a biotinylated donkey anti-rabbit (1:500; Jackson Immunoresearch).

2.2.3.2 Orexin innervation of PVT neurons projecting to the NacSh

Sections of the PVT were incubated in a cocktail of goat anti-orexin-A (1:2,000; Santa Cruz, catalogue #sc-8070, lot #I2302), and rabbit anti-FG (1:10,000). Tissue was then transferred to a biotinylated donkey anti-goat secondary antibody (1:500), incubated in ABC prepared according to kit directions, and reacted in DAB with nickel intensification. Sections were transferred to a biotinylated donkey anti-rabbit secondary antibody (1:500), and the ABC and DAB steps were completed as before but without nickel intensification.

2.2.3.3 CART innervation of PVT neurons projecting to the NacSh

Sections of the PVT were incubated in a rabbit anti-CART (1:5,000; Phoenix Pharmaceuticals, Inc., Belmont, CA, catalogue #H-003-62, lot #00324) primary antibody. Tissue was then transferred to a biotinylated donkey anti-rabbit secondary antibody (1:500), incubated in ABC prepared according to kit directions, and reacted in DAB with nickel intensification. Sections were incubated in a rabbit anti-FG (1:10,000) primary antibody and transferred to a biotinylated donkey anti-rabbit secondary antibody (1:500). The ABC and DAB steps were completed as before but without nickel intensification.

2.2.4 Immunofluorescence

2.2.4.1 Neuropeptide fiber co-localization with synaptophysin

To investigate if orexin and CART fibers co-localize with immunoreactivity for synaptophysin, a synaptic protein involved in exocytotic release, sections of the PVT were incubated in a primary antibody cocktail consisting of mouse anti-synaptophysin (1:500; Chemicon) and either goat anti-orexin-A (1:2,000) or rabbit anti-CART (1:3,000). Tissue was then transferred to a secondary antibody cocktail of Cy5-conjugated donkey anti-mouse and either Cy3-conjugated donkey anti-goat or Cy5-conjugated donkey anti-rabbit (1:500; Jackson Immunoresearch).

2.2.4.2 Orexin innervation of PVT neurons projecting to the NacSh

Sections of the PVT were incubated in a cocktail of goat anti-orexin-A (1:2,000) and rabbit anti-FG (1:10,000) primary antibodies. Tissue was then transferred to a secondary antibody cocktail of Cy3-conjugated donkey anti-goat and Cy2-conjugated donkey anti-rabbit (1:500).

2.2.4.3 CART innervation of PVT neurons projecting to the NacSh

Sections of the PVT were incubated in a cocktail of rabbit anti-CART (1:3,000) and goat anti-CTb (1:10,000) primary antibodies. Tissue was then transferred to a secondary antibody cocktail of Cy3-conjugated donkey anti-rabbit and Cy2-conjugated donkey anti-goat (1:500).

2.2.4.4 Orexin and CART innervation of PVT neurons projecting to the NacSh

Sections of the PVT were incubated in a cocktail of rabbit anti-CART (1:3,000) mouse anti-orexin (1:1,000; Alpha Diagnostic International, San Antonio, TX, catalogue #OXA15-M, lot #40514A), and goat anti-CTb (1:10,000) primary antibodies. Tissue was then transferred to a secondary antibody cocktail of Cy3-conjugated donkey anti-rabbit, Cy5-conjugated donkey anti-mouse, and Cy2-conjugated donkey anti-goat (1:500).

2.2.4.5 Orexin and CART innervation of PVT cells filled with neurobiotin

Sections of the PVT from animals receiving the neurobiotin injections were incubated in either a goat anti-orexin (1:1,000) or a rabbit anti-CART (1:5,000) primary antibody. Tissue was then transferred to either Cy2 conjugated donkey anti-goat (for orexin fibers) or Cy2 conjugated donkey anti-rabbit (for CART fibers) in a cocktail along with TRITC-conjugated Streptavidin (1:500; Jackson Immunoresearch).

2.2.5 Imaging

The present study used both low and high magnification imaging to examine the anatomical relationship between neuropeptide fibers and neurons projecting to the NacSh. Low magnification images were captured at three different rostrocaudal levels of the PVT. The Cy2 and Cy3 fluorophores were captured separately using a conventional fluorescence microscope (BX 51, Olympus) equipped with the appropriate filter cubes (U-MNB2 and U-MNG2, Olympus). The separate images of neuropeptide fibers and retrogradely labeled cells were then merged in Adobe Photoshop 5.5. A light microscope was also used to capture images of sections stained with DAB as the chromogen. High magnification images of orexin and CART fibers innervating retrogradely labeled PVT neurons were obtained with a 100x oil immersion lens. Images were captured and imported into Photoshop to improve contrast.

Confocal microscopy (FV300 scan head, BX50WI upright microscope; Olympus) was employed to investigate the presence or absence of neuropeptide fiber appositions onto retrogradely labeled PVT neurons. The confocal microscope was equipped with blue argon (488 nm), green helium neon (543 nm), and red helium neon (633 nm) lasers. High magnification images were captured with 100x oil-immersion objective lens and a zoom setting of 3x. All double labeled sections were scanned at 0.4 μm steps except the neurobiotin-stained tissue. Corresponding single optical sections for each fluorophore were subsequently combined in Adobe Photoshop 5.5 where brightness and contrast were adjusted. Each fluorophore was assigned to a particular RGB channel within Photoshop

in order to generate those color combinations that resulted in optimal contrast. Sections labeled with three fluorophores were scanned at 1.0 μm steps and were visualized as a small stack of optical sections.

Sections of the PVT treated with neurobiotin were imaged with the confocal microscope setup as described above. The neurobiotin signal and either the orexin or CART signal were imaged through 3 - 5 optical sections of 1 μm each. For each pseudo-section, the neurobiotin-filled cell and any neuropeptide fiber contacts were isolated from the background in Adobe Photoshop. These cut images were then stacked together to give the appearance of an isolated cell receiving multiple fiber contacts. The background was removed to clearly show contacts on the soma and dendrites of a single PVT neuron without interference from the dense background staining.

2.3 Effect of PVT stimulation on dopamine levels in the NacSh

2.3.1 Surgery

Rats were anesthetized with urethane (1.6 mg/kg, i.p.) and placed in a Kopf stereotaxic frame. The femoral vein was cannulated in a few animals for apomorphine administration. Body temperature was maintained at 37 °C using a Deltaphase isothermal heating pad (Braintree Scientific, Inc.). A hand drill was used to make holes overlying the striatum and diencephalon. Stimulating and recording electrodes (see below) were lowered into the thalamus and NacSh, respectively. The stimulating electrode was always

inserted on a 10 degree angle from the midline to avoid puncturing the mid-sagittal sinus. An Ag/AgCl reference electrode was inserted in the left hemisphere of all animals through a small hole drilled 7-8 mm posterior to bregma. All stereotaxic coordinates were derived from a rat brain atlas (Paxinos & Watson, 2005) and are described in more detail below.

2.3.2 Electrochemical detection

The Nafion-coated carbon fiber electrodes (30 μm tip diameter × 150 μm length, Quanteon, Nicholasville, KY) used in the present study to monitor dopamine release have been shown to provide excellent selectivity for dopamine over ascorbic acid and dihydroxyphenylacetic acid (Gerhardt & Hoffman, 2001). A new electrode was used for each animal and all electrodes were calibrated *in vitro* prior to experimentation. An electrode was used only if it responded in a highly linear fashion ($r^2 > 0.98$) to 2.5 μM additions of dopamine up to 10 μM while demonstrating at least a 100:1 selectivity for dopamine over ascorbic acid and DOPAC *in vitro*. The limit of detection for dopamine was defined as the concentration required to produce a response with a signal-to-noise ratio of 3:1. Amperometric recording of dopamine was performed by applying a 700 mV potential (vs. Ag/AgCl) to a carbon fiber electrode which was connected to a head stage pre-amplifier and sent to a computer-controlled instrument (FAST-16, Quanteon, L.L.C., Nicholasville, KY). Recordings were acquired at a sampling rate of 1 Hz. High speed chronoamperometric recordings were carried out by applying square wave pulses (0 to

550 mV vs. Ag/AgCl) to the carbon fiber electrode for 100 ms at 5 Hz. Pre-calibration revealed the detection limits for amperometry to fall between 5 and 15 nM and frequently exceed 50 nM for high-speed chronoamperometry. Since constant potential amperometry was found to yield the best signal-to-noise ratio, it was used for the majority of recordings (addressed further in *results*). Chemical specificity of the signal was also confirmed to be dopamine by examining the reduction/oxidation (red/ox) ratio from recordings done using high-speed chronoamperometry.

2.3.3 Effect of thalamic stimulation on oxidation current in the NacSh.

A concentric bipolar stimulating electrode (SNE-100, Rhodes Medical Instruments, Summerland, CA) was lowered dorsal to the thalamus (approximately 4.5 mm ventral to the brain surface). Monophasic current pulses were applied (1.0 ms pulses at 40 Hz for 5 s) and dopamine release was monitored in the NacSh. Pilot experiments indicated these stimulation parameters to be optimal to evoke an electrochemical signal in the NacSh using amperometry and chronoamperometry. The stimulating electrode was gradually lowered through the thalamus in 200 μm increments, with stimulation occurring at each site. Electrochemical events were saved and the corresponding thalamic stimulation coordinate was carefully noted for future histological identification. For each animal, 2-5 tracts were made through various anteroposterior and mediolateral regions of the thalamus. Anteroposterior coordinates ranged from 1.0 mm to 3.2 mm posterior to bregma and mediolateral coordinates ranged from 0.0 to 2.0 mm to the left and 0.0 to 1.0

mm to the right of the mid-sagittal sinus. Each experiment was terminated by passing a positive direct current (800 μA, 10 - 15 s) through the carbon fiber electrode. These current parameters produced a small lesion at the electrode tip, facilitating histological verification of the recording site.

Animals were perfused transcardially using 150 ml of heparinized saline followed by 500 ml of 10% formalin. Brains were removed and post-fixed in 10% formalin overnight. Sections were cut at 100 μm on a vibratome, mounted on gelatin-coated slides, and stained using a standard Nissl stain. Sections were then examined with a microscope (BX 51, Olympus) to determine the placement of the carbon-fiber electrode within the NacSh as well as the ventral-most site of each tract made by the stimulating electrode in the thalamus. Each stimulation site was identified by estimating the location of each 200 μm increment dorsal to the damage made by the electrode tip. A stimulation site in the thalamus was considered to evoke a response in the NacSh if the recorded current increase occurred following the onset of stimulation and peaked above the limit of detection. Responses were converted to represent a change in dopamine concentration based on pre-calibration data for each microelectrode.

2.3.4 Effect of nomifensine on the PVT-evoked oxidation current in the NacSh.

Five animals were used to determine if the properties of the observed electrochemical signal were sensitive to the dopamine uptake inhibitor nomifensine. The stimulating electrode was placed in the posterior PVT (3.2 mm posterior to bregma and

immediately to the left hemisphere avoiding the mid-sagittal sinus) while the recording electrode was placed in the medial shell of the nucleus accumbens (1.1 mm anterior and 1.1 mm lateral to bregma and 7.0 mm below the brain surface). If necessary, the electrodes were adjusted in the dorsal-ventral direction to find a response exceeding the detection limit. Typically, a response was found within one or two adjustments of the stimulating electrode. Subjects were injected with the dopamine uptake inhibitor nomifensine (20 mg/kg, i.p.). The PVT was stimulated once every 5 minutes thereafter and electrochemical activity in the NacSh was monitored as before. Animals were perfused at the end of the experiment and tissue was processed as in section 2.3.3.

2.3.5 Effect of intra-VTA lidocaine on PVT-evoked oxidation current in the NacSh

Four animals were used to investigate whether the observed electrochemical event evoked by PVT stimulation is dependent on the firing of dopamine neurons in the VTA. The coordinates detailed in section 2.3.4 were used to stimulate the PVT and record events in the NacSh. A pipette (50 – 75 μm O.D.) filled with 4% lidocaine was centered above the VTA 5.0 mm posterior and 1.1 mm lateral to bregma. The pipette was lowered approximately 1.0 mm into the cortex while a PVT-evoked response was found to assure that any diffusion from the pipette had no effect on the initial electrochemical recordings. When a stimulation site was found, the pipette was lowered 8.5 - 9.0 mm below the brain surface and another 2 – 3 PVT-evoked responses were recorded before lidocaine infusion. A total of 2 μl of lidocaine was infused over a three minute period into the VTA

using a pressure injection device (Harvard Apparatus, Holliston, MAS). The volume ejected was determined by carefully observing the position of the meniscus in the micropipette. The PVT was stimulated every 5 minutes following lidocaine administration and electrochemical measurements were recorded in the NacSh. Animals were perfused and tissue was processed for histological verification.

2.3.6 Effect of kynurenic acid on PVT-evoked oxidation current in the NacSh

Six animals were used to investigate the contribution of local glutamate receptors to PVT-evoked electrochemical currents recorded in the NacSh. Kynurenic acid was used as a broad spectrum glutamate receptor antagonist at NMDA, AMPA, and kainate receptors (Stone, 1993). A recording electrode and a glass pipette filled with kynurenic acid (O.D. 50-75 μm) were both lowered over bregma, with the pipette angled at 10 degrees from the midline. The pipette was inserted into the brain 1.2 mm anterior, 2.4 mm lateral to bregma, and 7.1 mm ventral to the brain surface. The electrode was then lowered 1.2 mm anterior, 1.1 mm lateral to bregma, and 7.0 mm ventral to the brain's surface. Histological analysis indicated that there was a range of 200 – 400 μm between the tip of the pipette and recording electrode. A stimulating electrode was then placed in the PVT and an electrochemical response was evoked in the NacSh as described in section 2.3.4. A PVT-evoked event was recorded every 5 minutes for 15 minutes and followed by an infusion of 50 mM kynurenic acid. The PVT was stimulated every 5 minutes following kynurenic acid application and electrochemical activity was recorded

in the NacSh as before. Control experiments were done in the same animals as the kynurenic acid experiments with three animals receiving saline before kynurenic acid and three animals receiving kynurenic acid before saline. Both treatments were infused at a volume of 500 nl over 3 minutes. At least two hours were allotted between injections so that any effect observed by the initial treatment had time to recover.

Since kynurenic acid did not fully block the response, further experiments examining the role of dopamine cell firing were carried out. The effects of apomorphine, a mixed dopamine agonist known to have inhibitory effects by acting on autoreceptors located on dopamine neurons (Grace & Bunney, 1983), on PVT-evoked responses were examined in four of the six animals used in the kynurenic acid experiments. The effects of apomorphine could be reliably tested in the same rats due to the full recovery of PVT-evoked electrochemical events within an hour following kynurenic acid application. Apomorphine (0.15 mg/kg; i.v.) was delivered at a rate of 1 ml/minute. PVT-evoked events were recorded before apomorphine administration and every 5 minutes thereafter. Animals were perfused at the end of the experiment and tissue was processed as described in section 2.3.3.

2.3.7 Anterograde tracing

Six rats were anesthetized with equithesin (0.3 ml/100g, i.p.) and placed in a Kopf stereotaxic frame. Iontophoretic injections of 2% biotinylated dextran amine (BDA; Sigma) dissolved in PBS were performed by applying a 5-6 μA positive current (7s on/off for 30 minutes) through a chlorinated silver wire placed in a glass pipette (7-10 μm tip diameter). The coordinates used for injecting BDA into various anteroposterior regions of the PVT were as follows: 1.0 or 3.0 mm posterior and 0.8 mm lateral to bregma (angled at 10° from the midline), and 5.0 mm ventral to the dura. The scalp incision was sutured and rats were returned to their home cages for recovery. Following a 10-14 day postoperative survival, rats were deeply anesthetized with equithesin (0.4 ml/100g, i.p.) and perfused with 150 ml heparinized saline followed by 450-500 ml ice-cold 4% paraformaldehyde. The brains were removed, post-fixed for 2-4 hours, and cryoprotected in graded sucrose concentrations (10% and 20% w/v). Brains were then frozen using Fisherbrand Histo-freeze and sections from the nucleus accumbens and thalamus were taken at 50 μm and collected in PBS. Brain sections were incubated in ABC overnight at 4 °C. After a few rinses, the tissue was reacted for 5-10 minutes with diaminobenzidine (DAB) with nickel intensification to produce black BDA labeling. Sections were then stained for tyrosine hydroxylase (TH) by incubating in mouse monoclonal anti-TH (Sigma; 1:100,000) overnight at 4°C followed by an ABC/DAB reaction without nickel intensification as described above. Sections were examined using a standard light microscope (Olympus BX51) equipped with a digital camera (SPOT RT

Slicer, Diagnostic Instruments Inc, Sterling Heights, MI) and images were captured and transferred to Adobe Photoshop 5.5 to optimize light and contrast levels.

2.3.8 Chemicals and Drugs

Nomifensine, lidocaine, and kynurenic acid were all purchased from Sigma (St. Louis, MO, USA). Chemicals were dissolved in 0.9% saline with the exception of the kynurenic acid which was dissolved first in a drop of sodium hydroxide and then diluted with saline. Hydrochloric acid was used to adjust the pH of the kynurenic acid solution to 7.4.

2.3.9 Data Analysis

All voltammetric signals were analyzed by converting each recorded current to a concentration based on pre-calibration responses to known concentrations of dopamine. The events observed in the present studies were brief, usually returning to baseline within 20 seconds. To account for baseline drift, inherent in voltammetric recording methods, a new baseline was established for each response by averaging 4 data points prior to PVT stimulation. Oxidation current changes caused by PVT stimulation were calculated as a change from baseline which was then converted to a concentration value. A paired t-test was used to compare the average peak and clearance rate of dopamine signals before and after both nomifensine and lidocaine infusion. A single factor analysis of variance was

used to examine the effect of kynurenic acid and apomorphine on dopamine peak values at various time points following drug administration. Post-hoc comparisons were made using Tukey's test.

Chapter 3

Results

3.1 Results Summary: Anatomy

The anatomical findings of the present thesis demonstrate that the PVT contains the highest density of orexin and CART immunopositive fibers when compared to adjacent thalamic nuclei. Both fiber types typically co-expressed immunoreactivity for the synaptic marker synaptophysin suggesting that orexin and CART are released from vesicles within the PVT. The PVT was the only thalamic region to receive a dense innervation from both the orexin and CART peptides while exhibiting dense retrograde labeling from the NacSh. High magnification confocal imaging revealed orexin and CART fiber varicosities within the PVT made frequent putative contacts with the soma and proximal dendrites of PVT neurons projecting to the NacSh.

3.2 Orexin and CART innervation of PVT neurons projecting to the NacSh

3.2.1 Orexin fiber innervation of the midline and intralaminar thalamus

A high density of orexin fiber immunoreactivity was observed throughout the anteroposterior extent of the PVT (Fig. 3) with the heaviest innervation occurring in more posterior regions (Fig. 3E). The shape of the PVT changes in posterior regions to occupy a greater proportion of thalamic tissue immediately lateral to the midline. The observation that orexin fiber immunoreactivity patterns follow this change in shape suggests that antibodies against the orexin-A peptide can be used to distinguish the PVT from adjacent nuclei. Orexin fiber immunoreactivity was found to be weak in the paratenial nucleus which is located lateral to the PVT in anterior sections (Fig. 3 A, B). A moderate density of orexin fibers were found in the intermediodorsal nucleus which is located ventral to the PVT in posterior sections (Fig. 3 D, E). There was a considerable orexin fiber presence within the centromedial nucleus, with heavier staining observed in more posterior sections (Fig. 3 C-E). A barely detectable level of orexin fiber immunoreactivity was found in the mediodorsal and paracentral nuclei (Fig. 3 C-E). Examination of orexin fibers in the PVT at high magnification (Fig. 3 F) revealed unevenly spaced fiber swellings of various sizes which are characteristic of en passant enlargements. Thick branched and un-branched fibers with a beaded appearance ran in all directions with fibers often terminating in a cluster of beads.

Fig. 3. The photomicrographs in panels A to E show the distribution of orexin-like immunoreactive fibers in the paraventricular nucleus of the thalamus (PVT). The shape of the PVT varies slightly throughout its anteroposterior extent but is well defined at each level by heavy orexin immunoreactivity. In general, the PVT is easily distinguished from adjacent thalamic nuclei by dense orexin innervation. Numbers indicate approximate distance from bregma. Panel F shows fibers and swellings in the PVT immunostained for orexin and captured under 100X oil immersion lens. AN, anterior nucleus of the thalamus; CM, centromedial nucleus of the thalamus; Hb, habenula; IMD, intermediodorsal nucleus of the thalamus; MD, mediodorsal nucleus of the thalamus; PC, paracentral nucleus of the thalamus; PT, paratenial nucleus of the thalamus; PVA, anterior paraventricular nucleus of the thalamus; PVP, posterior paraventricular nucleus of the thalamus; PVT, paraventricular nucleus of the thalamus; sm, stria medullaris

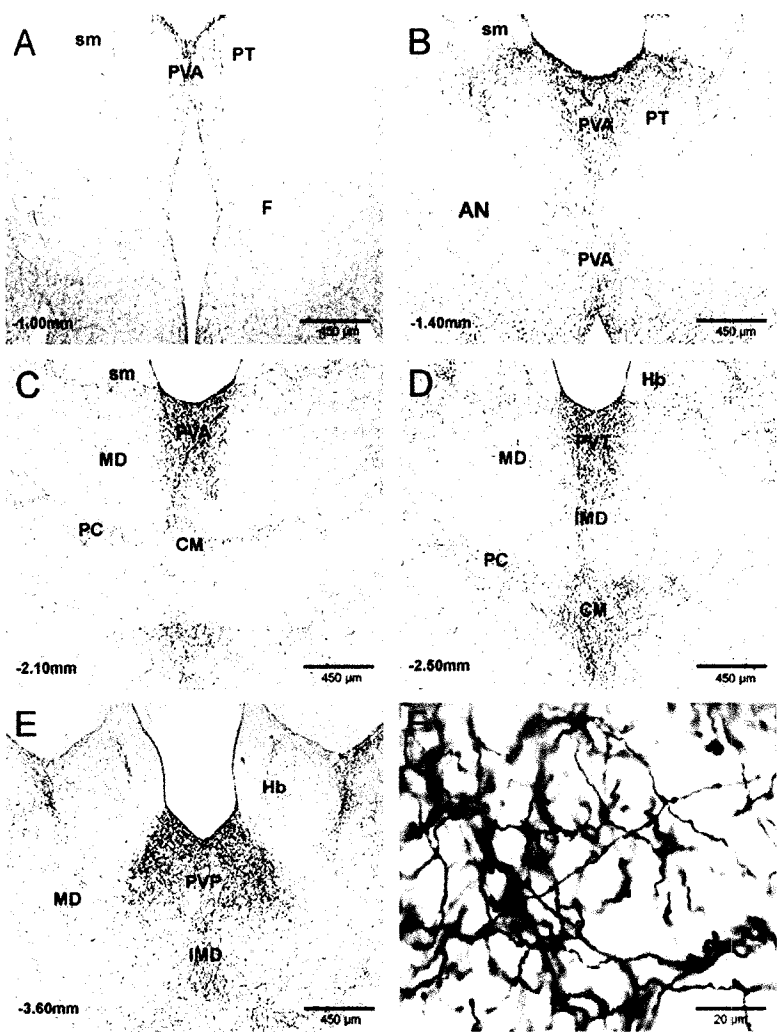
A
sm
PT
PVA
F
-1.00mm
450 µm
B
sm
PVA
PT
AN
PVA
-1.40mm
450 µm
C
sm
PVA
MD
PC
CM
-2.10mm
450 µm
D
Hb
MD
IMD
PC
CM
-2.50mm
450 µm
E
Hb
PVP
MD
IMD
-3.60mm
450 µm
F
20 µm

3.2.2 CART fiber innervation of the midline and intralaminar thalamus

A high density of CART fiber immunoreactivity was observed throughout the anteroposterior extent of the PVT (Fig. 4) with the heaviest innervation seeming to occur, as seen with orexin fibers, in more posterior regions (Fig. 4 D, E). Furthermore, the rostrocaudal shape of the PVT (described in 3.2.1) is closely followed by CART fiber immunoreactivity suggesting that antibodies against CART can be used to distinguish the PVT from adjacent nuclei, as was the case with orexin. CART fiber immunoreactivity was found to be weak in the paratenial, centromedial and intermediodorsal nuclei (Fig. 4 A-E), and slightly above background levels in the mediodorsal nucleus. The anterior thalamic nucleus contained moderate CART fiber immunoreactivity throughout (Fig. 4 B-D), as previously described (Koylu *et al.*, 1998). Examination of CART fibers in the PVT at high magnification (Fig. 4F) revealed a high density of en passant enlargements suggestive of transmitter release. As with orexin, thick branched and un-branched CART fibers with a beaded appearance ran in all directions with fibers often terminating in a cluster of beads.

Fig. 4. The photomicrographs in panels A to E show the distribution of CART-like immunoreactive fibers in the paraventricular nucleus of the thalamus (PVT). The shape of the PVT varies slightly throughout its anteroposterior extent but is well defined at each level by heavy CART immunoreactivity. In general, the PVT is easily distinguished from adjacent thalamic nuclei by dense CART innervation. Numbers indicate approximate distance from bregma. Panel F shows fibers and swellings in the PVT immunostained for CART and captured under 100X oil immersion lens. AN, anterior nucleus of the thalamus; CM, centromedial nucleus of the thalamus; Hb, habenula; IMD, intermediodorsal nucleus of the thalamus; MD, mediodorsal nucleus of the thalamus; PC, paracentral nucleus of the thalamus; PT, paratenial nucleus of the thalamus; PVA, anterior paraventricular nucleus of the thalamus; PVP, posterior paraventricular nucleus of the thalamus; PVT, paraventricular nucleus of the thalamus; sm, stria medullaris

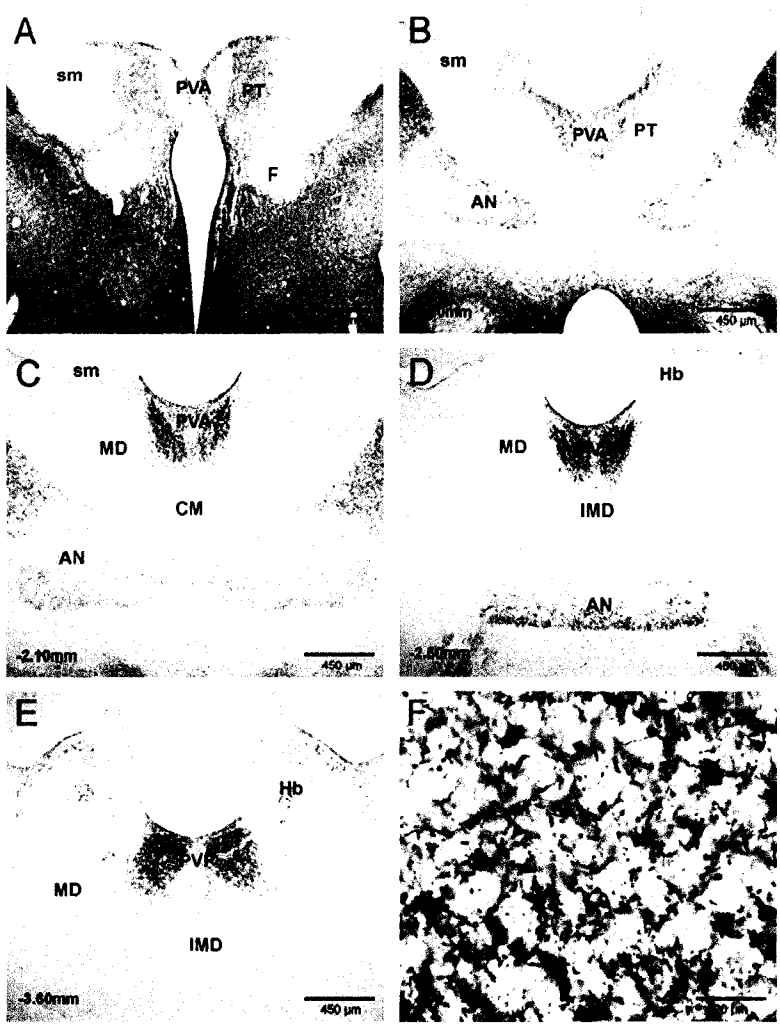
A
sm
PVA
PT
F
B
sm
PVA
PT
AN
450 µm
C
sm
PVA
MD
CM
AN
-2.10mm
450 µm
D
Hb
MD
IMD
AN
E
Hb
MD
IMD
-3.60mm
450 µm
F

3.2.3 Neuropeptide fiber co-localization with synaptophysin

Immunofluorescent experiments were carried out to investigate whether orexin and CART immunoreactive fibers co-localize with synaptophysin, a synaptic vesicle protein involved in vesicular release from terminals. Both fiber types were found to co-express synaptophysin immunoreactivity on axonal terminals and enlargements throughout the anteroposterior and mediolateral extent of the PVT (Fig. 5). Examination of 0.4 μm optical sections of sequential scans of the PVT revealed considerable synaptophysin presence within enlargements of labeled fibers. The overlap between orexin and synaptophysin and CART and synaptophysin was consistently found on the enlargements and not on segments of fibers between enlargements.

3.2.4 Location of retrograde tracer deposits in the NacSh

Retrograde tract tracing experiments were done to label thalamic neurons projecting to the NacSh. Only those animals with tracer injection largely restricted to the shell region of the nucleus accumbens were used in the present experiments. As shown in Figure 6, the dense cores of the injections were found in the anterior, middle, and posterior aspects of the medial NacSh. These locations throughout the NacSh cover the extent of the nucleus accumbens which have been previously described to receive afferents from the PVT (Moga *et al.*, 1995).

Fig. 5. Representative case demonstrating that orexin (A-C) and CART (D-F) fiber varicosities typically co-express immunoreactivity for synaptophysin (arrows, C, F), a protein that has been used as a reliable marker of synaptic vesicle release. Typically, double labeling was confined to the swellings of immuno-labeled fibers rather than the intervaricose segments. Each image represents a single optical section of 0.4 μm captured using confocal microscopy. Syp, synaptophysin.

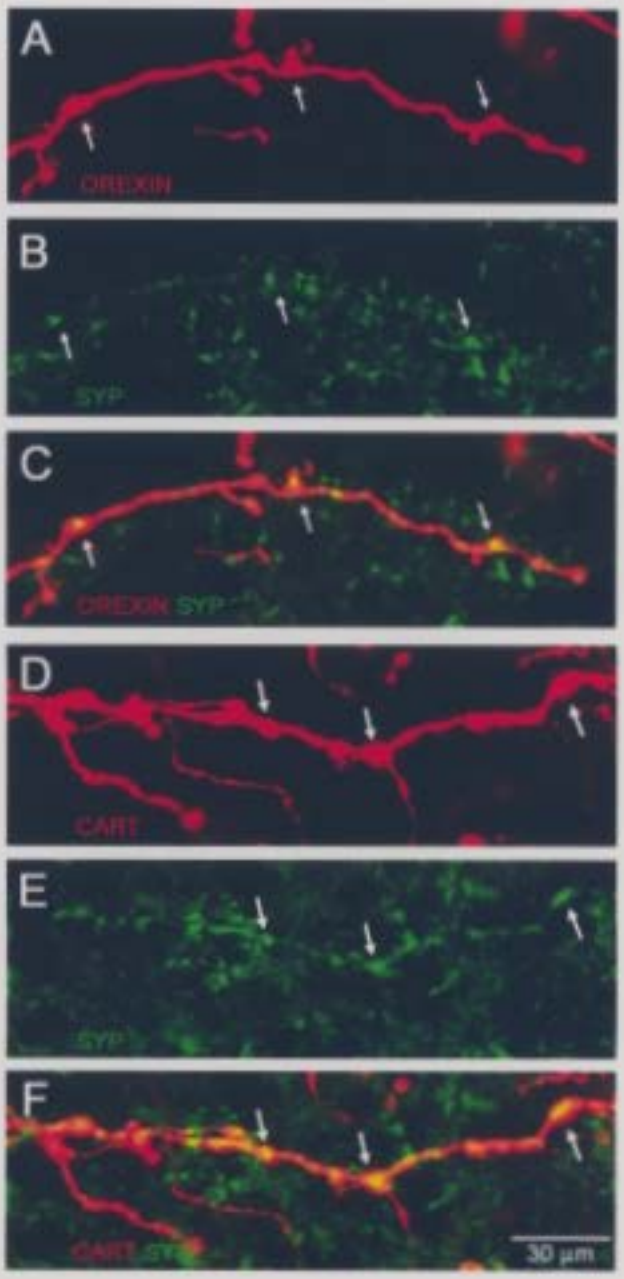
A
OREXIN
B
SYP
C
OREXIN SYP
D
CART
E
SYP
F
30 µm

Fig. 6. Approximate location of 6 fluorogold (A) and 4 cholera toxin b injections (B). The rostrocaudal levels shown are the ones at which the tracer immunoreactivity was the strongest. The majority of injections from both tracers were restricted to the dorsomedial nucleus accumbens shell (NacSh). Numbers represent approximate distance anterior to bregma. ac, anterior commissure; NacC, nucleus accumbens core.

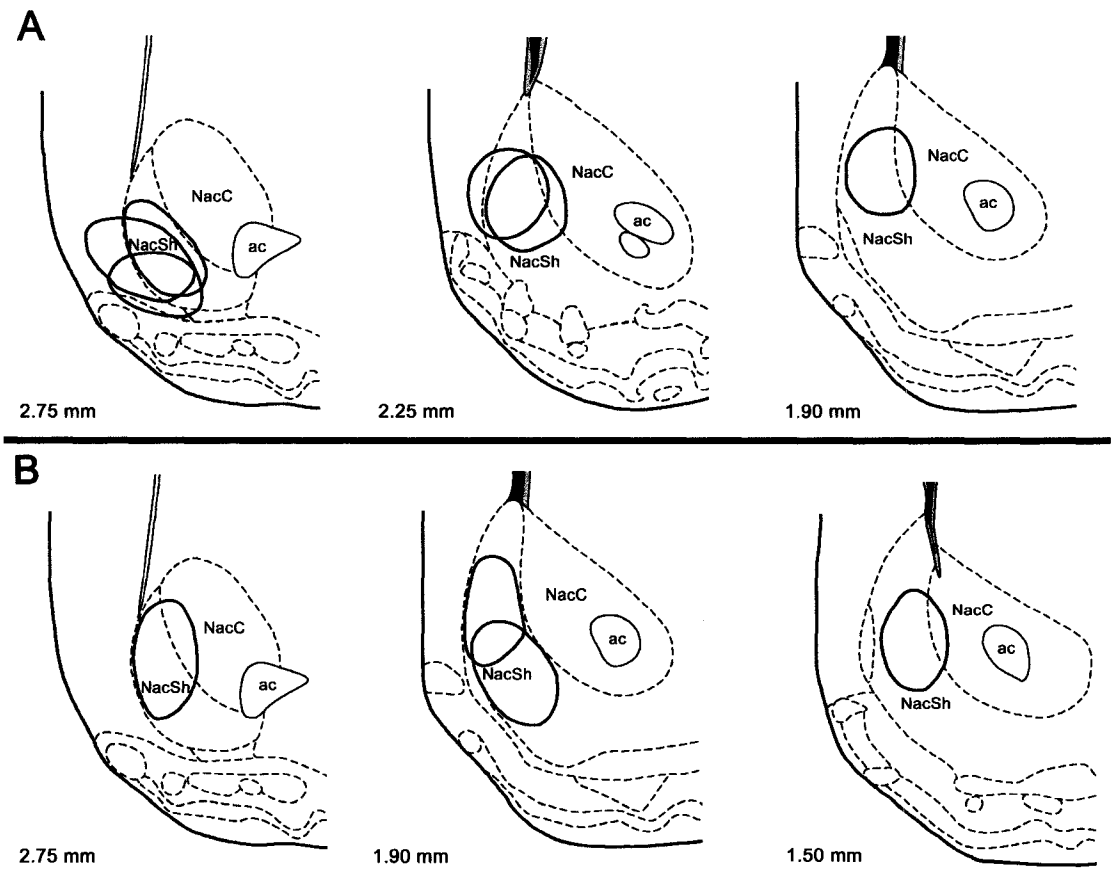
A
NacC
NacSh
ac
2.75 mm
NacC
ac
NacSh
2.25 mm
NacC
ac
NacSh
1.90 mm
B
NacC
NacSh
ac
2.75 mm
NacC
ac
NacSh
1.90 mm
NacC
ac
NacSh
1.50 mm

3.2.5 Overlap between orexin and CART immunoreactivity and thalamic neurons projecting to the NacSh

Immunofluorescent labeling of orexin and CART fibers in the midline and intralaminar thalamus provide the same specificity as observed using DAB as the chromogen (see sections 3.2.1 and 3.2.2). Dense immunoreactivity for orexin (Fig. 7 D-F) and CART (Fig. 7 G-I) was observed to concentrate medially beneath the third ventricle in anterior sections (Fig. 7 D, G) and extend laterally in posterior sections (Fig. 7 F, I). The locations of neurons retrogradely labeled from the NacSh followed this pattern of fiber immunoreactivity, demonstrating that the majority of thalamic neurons projecting to the NacSh are found within the boundaries of the PVT. Dense fiber staining was not common to the entire midline and intralaminar thalamus as regions adjacent to the PVT exhibited little or no staining at all. The paratenial nucleus was the only other thalamic nucleus to exhibit CTb-positive neurons but this nucleus was largely devoid of orexin and CART fiber staining (Fig. 7 D, G).

Fig. 7. Fluorescent images showing the distribution of retrogradely labeled cells in the paraventricular nucleus of the thalamus (PVT) following cholera toxin b (CTb) injection in the nucleus accumbens shell (A-C). Patterns of retrograde labeling largely overlapped immunofluorescence for orexin (OX, D-F) and CART fibers (G-I). This overlap was evident throughout the anterior (D, G), middle (E, H), and posterior (F, I) regions of the PVT. Numbers indicate approximate distance from bregma. 3V, 3rd ventricle; MD, mediodorsal nucleus; Pt; paratenial nucleus.

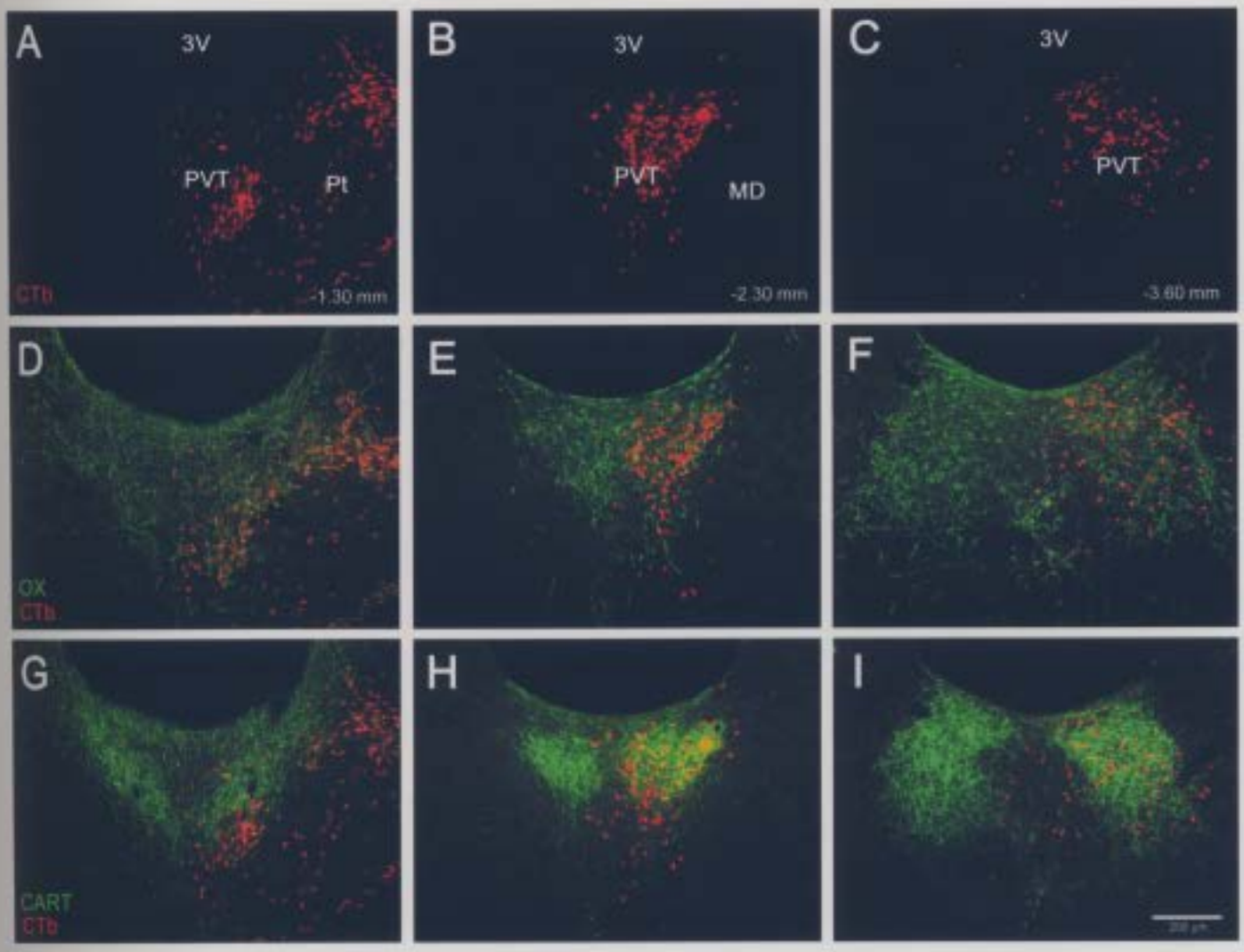
A
3V
PVT
Pt
CTb
-1.30 mm
B
3V
PVT
MD
-2.30 mm
C
3V
PVT
-3.60 mm
D
OX
CTb
E
F
G
CART
CTb
H
I

3.2.6 Orexin and CART fiber innervation of PVT neurons projecting to the NacSh

Orexin and CART fiber innervation of PVT cells retrogradely labeled from the nucleus accumbens were examined with high magnification light and confocal microscopy. Examination of sections stained with DAB revealed putative fiber contacts onto FG-positive cells (Fig. 8). These presumed contacts were easily identifiable in sections stained for orexin and FG (Fig. 8 A-C) as well as those stained for CART and FG (Fig. 8 D-F). Fibers were commonly seen to wrap around a labeled soma, sometimes appearing to terminate at a point near or on the cell body. Although no quantitative analysis was performed, it appeared that orexin and CART fibers formed a similar number of contacts onto labeled PVT neurons.

High magnification confocal images were collected at 0.4 μm steps to provide further evidence of appositional contacts. Figure 9 shows that both orexin (Fig. 9 A-C) and CART (Fig. 9 D-F) fiber appositions onto PVT neurons projecting to the NacSh are evident within single optical sections. Although the FG tracer generally labeled a greater proportion of individual PVT neurons when compared to CTb, neither FG nor CTb generated complete staining of both the soma and dendrites. Typically no more than half the cell body would show signs of immunofluorescence and dendritic staining was observed only in very rare cases. At best, a fiber could be seen apposing a dendrite approximately 10 μm away from the cell body (Fig.9 A, D), providing at least some evidence for the existence of axodendritic appositions as well as the more commonly observed axosomatic appositions.

Fig. 8. High magnification light microscope images showing putative fiber contacts onto neurons (brown) in the paraventricular nucleus of the thalamus (PVT) retrogradely labeled with fluorogold (FG) from the shell of the nucleus accumbens. Orexin (OX, A-C) and CART fibers (D-F) appear black from a nickel-intensified diaminobenzidine reaction. Arrows show fiber enlargements apposing labeled PVT neurons.

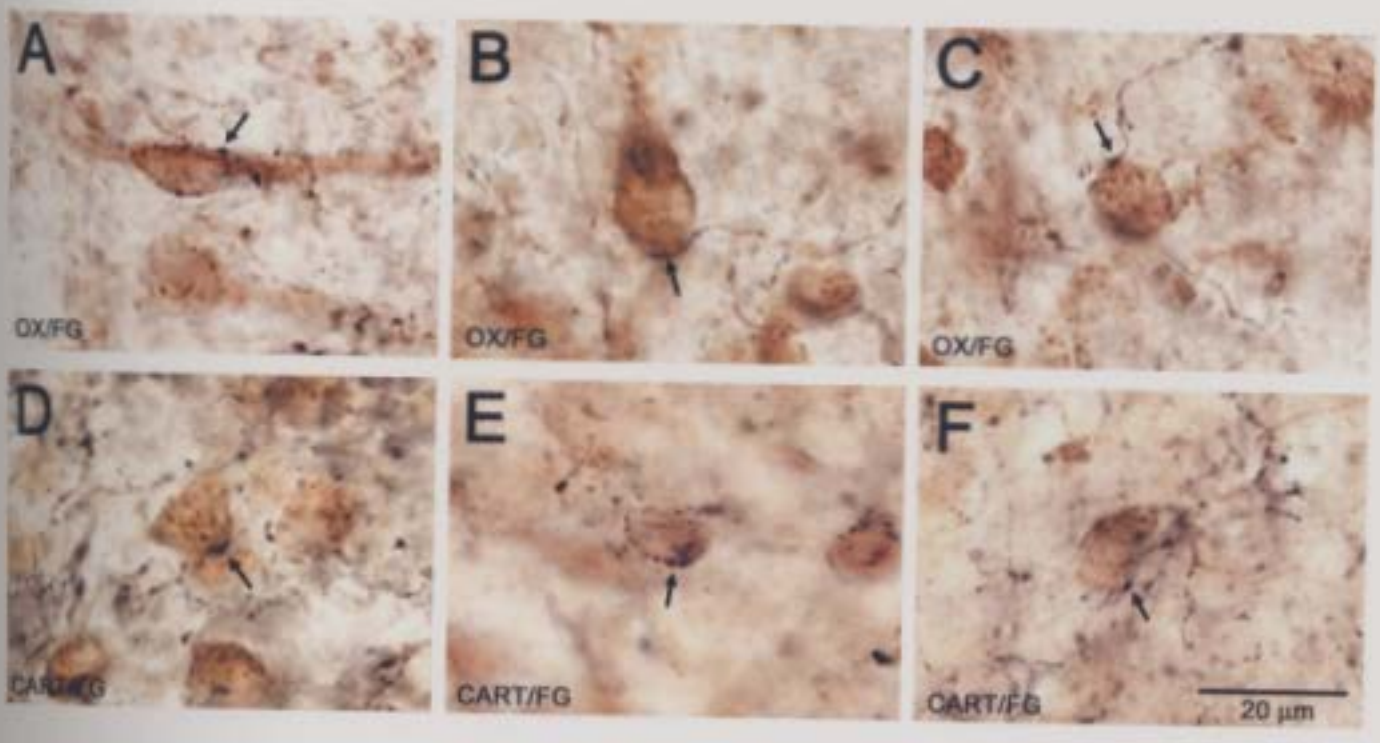
A
OX/FG
B
OX/FG
C
OX/FG
D
E
CART/FG
F
CART/FG
20 µm

Fig. 9. High magnification confocal images showing putative fiber contacts onto cells of the paraventricular nucleus of the thalamus (PVT) retrogradely labeled from the shell of the nucleus accumbens (red). Images shown are single 0.4 μm optical sections removed from a stack. Labeled PVT cells were commonly apposed by orexin (OX, green; A-C) and CART fibers (green, D-F). In a few cases where the retrograde tracer filled a proximal dendrite of a PVT cell, presumed axodendritic contacts were evident (arrowheads, A, D). Arrows show representative fiber contacts onto labeled PVT neurons.

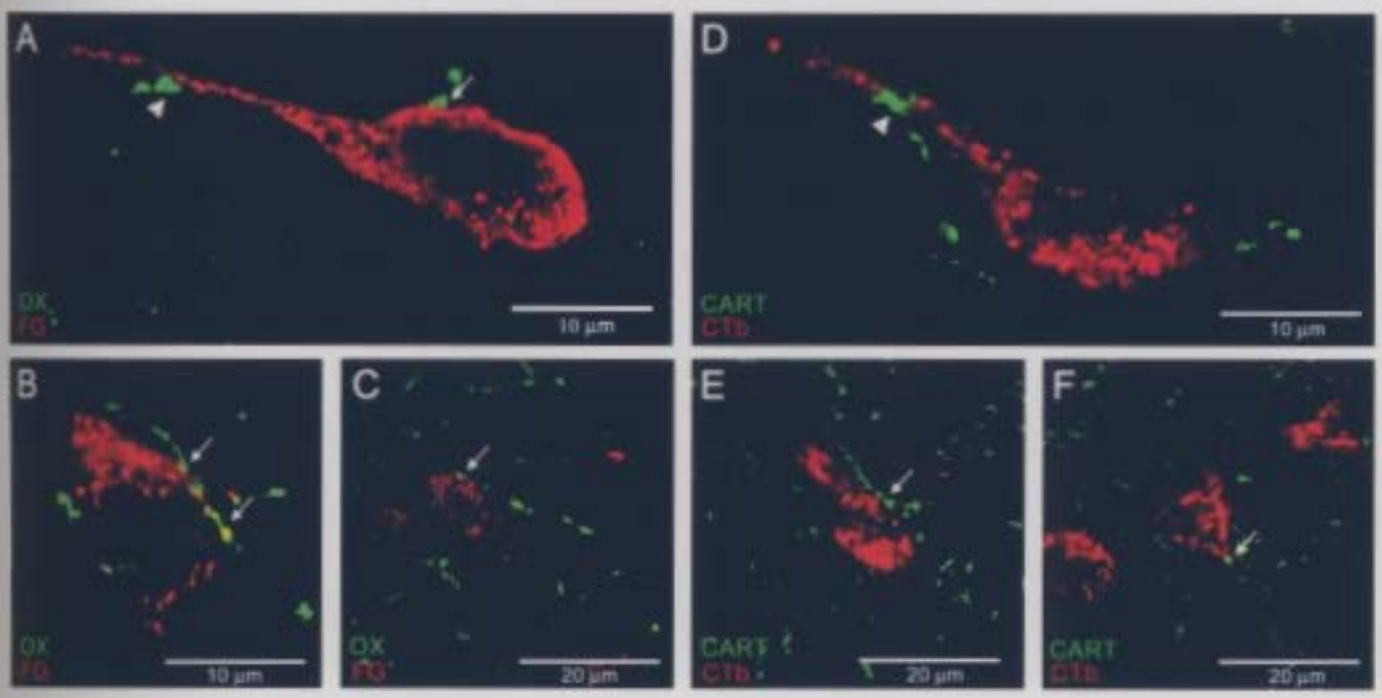
A
OX
FG
10 µm
D
CART
CTb
10 µm
B
OX
FG
10 µm
C
OX
FG
20 µm
E
CART
CTb
20 µm
F
CART
CTb
20 µm

Experiments were also performed to assess whether the same PVT neuron retrogradely labeled from the NacSh is apposed by both orexin and CART fiber types. Retrogradely labeled cells were scanned throughout the z-axis at 1.0 μm, and the same levels were sequentially scanned once again to capture both orexin and CART immunofluorescence. Due to the unlikely chance that both fiber types may appose a single CTb labeled cell within the same optical section, a series of three to five optical sections (1.0 μm steps) of the CTb signal alone was captured and stacked. The optical sections at which the orexin and CART contacts occurred were then superimposed on the CTb stack. Orexin and CART fibers were commonly seen apposing the same PVT neuron (Fig 10).

The full shape of a PVT neuron was much more readily identifiable following injection of neurobiotin into the PVT. Examination of neurobiotin-filled cells at the light microscopic level revealed that PVT neurons have short proximal dendrites that quickly taper to fine distal dendrites. We could capture confocal images of the neurobiotin-filled soma and proximal dendrites, but were unable to clearly visualize the distal dendrites of PVT neurons because of their very fine taper. By combining neurobiotin with orexin or CART immunofluorescence, numerous fiber contacts were seen on both the soma and proximal dendrites of PVT neurons. In cases of more complete filling of PVT neurons, evidence for both axosomatic and axodendritic appositions was seen in all PVT cells scanned and was noted for both orexin and CART fiber types (Fig. 11).

Fig. 10. High magnification confocal images demonstrating both orexin (OX, green) and CART fiber (blue) contacts onto a common PVT neuron (red) retrogradely labeled with cholera toxin b (CTb) from the nucleus accumbens. Each image represents a stack of 3 – 5 optical sections taken through the z-axis at 1.0 μm steps. Arrows show representative fiber contacts onto labeled PVT neurons.

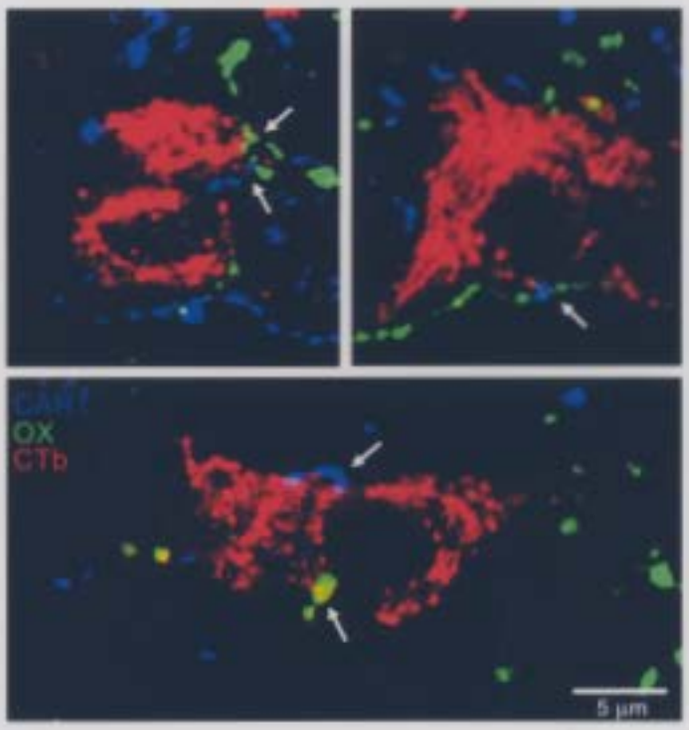
DAPI
OX
CTb
5 µm

Fig. 11. High magnification confocal images demonstrating the presence of orexin (green, A-C) and CART (green, D-F) fiber contacts onto both the soma and dendrites of filled neurons within the paraventricular nucleus of the thalamus (PVT). Neurobiotin (red) was iontophoretically applied into the PVT. Each image represents a stack of 3 – 5 optical sections taken though the z-axis at 1.0 μm steps.

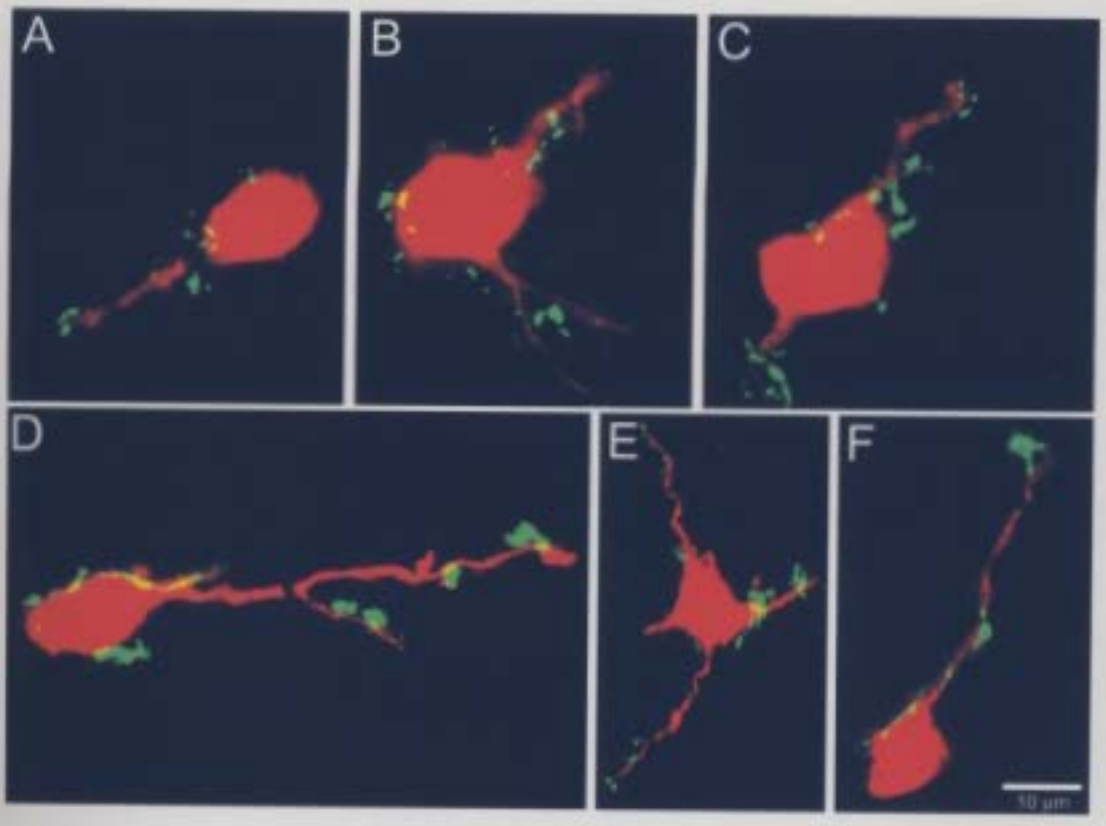
A
B
C
D
E
F
10 µm

3.3 Results Summary: Voltammetry

The voltammetry data demonstrate that electrical stimulation of the PVT resulted in a transient increase in an oxidation current within the NacSh which was characteristic of dopamine release. The PVT-evoked increases in NacSh oxidation current were not dependent on the firing of midbrain dopamine neurons as intra-VTA lidocaine and i.p. apomorphine administration had no effect on PVT-evoked responses. Furthermore, infusion of the ionotropic glutamate receptor antagonist kynurenic acid significantly attenuated the peak of PVT-evoked responses, suggesting that glutamate release from PVT terminals acts presynaptically to regulate tonic dopamine release.

3.4 Effect of PVT stimulation on dopamine levels in the NacSh

3.4.1 Selectivity of electrochemically-de`tected events

From the observation that the PVT is heavily innervated by numerous arousal related peptides including the orexins and CART, it was of interest to determine if the output of the PVT plays any role in modulating dopamine release within the NacSh. Initial voltammetry experiments using nafion-coated carbon fiber electrodes revealed an increase in oxidation current in the NacSh following PVT stimulation. Attempts were made to successfully record PVT-evoked responses using high-speed chronoamperometry. In many instances, a change in oxidation current clearly observed

using constant potential amperometry (Fig. 12A) was typically lower than the limit of detection for high-speed chronoamperometry (Fig 12B). Variations that were seen in the observed response size allowed chronoamperometric detection for some of the larger events. When a response was found using amperometry (Fig. 12C) that was above the limit of detection for chronoamperometry, the recording mode was switched to chronoamperometry and a red/ox ratio reflecting that of dopamine (0.7 - 0.8) was observed (Fig. 12D). However, the majority of events fell below the chronoamperometric detection limit and were much better recognized using amperometry (Fig. 12A) compared to chronoamperometry (Fig. 12B). Therefore, constant potential amperometry was used for the remainder of the experiments.

3.4.2 Effect of thalamic stimulation on oxidation current in the NacSh

Stimulation of specific regions of the midline and intralaminar thalamus generated a transient increase in oxidation currents within the NacSh. By lowering the stimulating electrode through multiple tracks at various anteroposterior and mediolateral levels of the thalamus, it was determined that stimulation of the PVT consistently evoked an increase in oxidation current in the NacSh whereas stimulation of adjacent nuclei did not (Fig. 13). Stimulation of the mediodorsal, lateral habenular and centromedial nuclei, as well as the stria medullarius and fasciculus retroflexus fiber tracts, resulted in no oxidation current change in the NacSh. Certain placements in the lateral aspect of the mediodorsal nucleus or the dorsal aspect of the intermediodorsal nuclei were found to evoke a NacSh response

Fig. 12. A transient electrochemical signal is observed in the NacSh following stimulation of the thalamus. Pilot data revealed certain placements to generate low magnitude responses (20-30 nM) which were more easily detected using constant potential amperometry (A) compared to high-speed chronoamperometry (B). A few cases were found in which the oxidation current change detected by amperometry (C) was large enough to be detected by chronoamperometry (solid line, D). For these cases, a rise in oxidation current was accompanied by a rise in reduction current (dotted line, D) which reflected a redox ratio typical of dopamine (0.7-0.8). Note the difference between electrochemical signals using amperometry (A, C) as compared to high-speed chronoamperometry (B, D). All current responses are translated to a concentration value based on pre-calibration data.

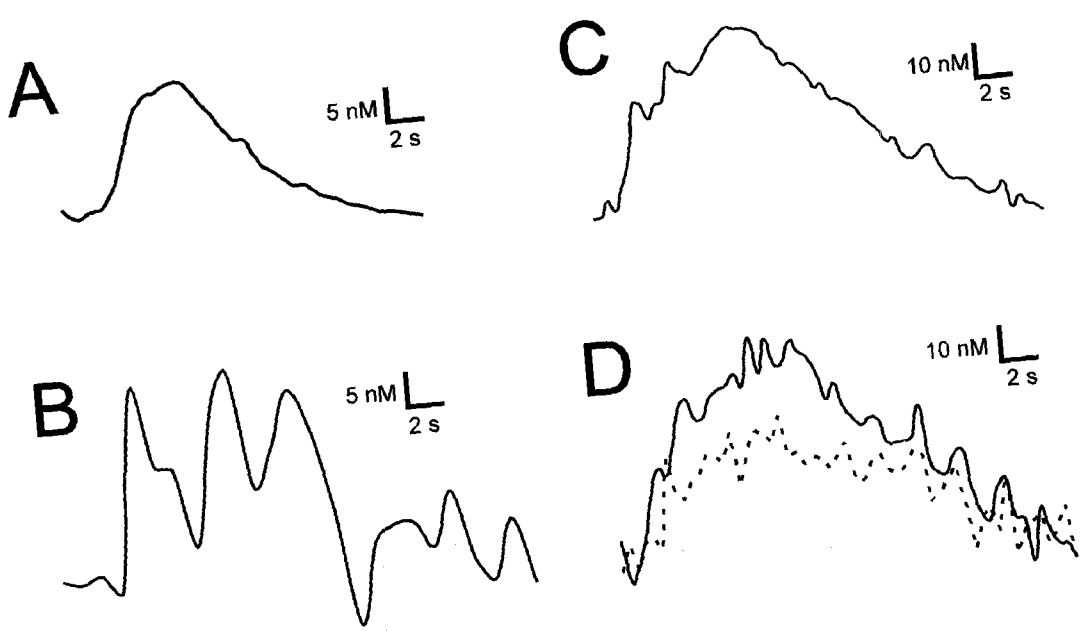
A
5 nM
2 s
C
10 nM
2 s
B
5 nM
2 s
D
10 nM
2 s

Fig. 13. Stimulation of the dorsal midline thalamus increased electrochemically detected dopamine in the nucleus accumbens shell (NacSh). Various thalamic nuclei (A) were stimulated while electrochemical current was monitored in the NacSh. Thalamic stimulation sites resulting in a transient NacSh dopamine oxidation current rising above a 3:1 signal-to-noise ratio concentrate within the paraventricular nucleus of the thalamus (PVT, filled circles, B). Stimulation of the adjacent mediodorsal (MD), centromedial (CM), and lateral habenular nuclei (LHb) did not raise the dopamine oxidation current in the NacSh (hollow circles). Carbon fiber electrode placements within the NacSh are shown for each of 9 subjects (C). Numbers indicate approximate distance anterior (+) and posterior (-) to bregma.

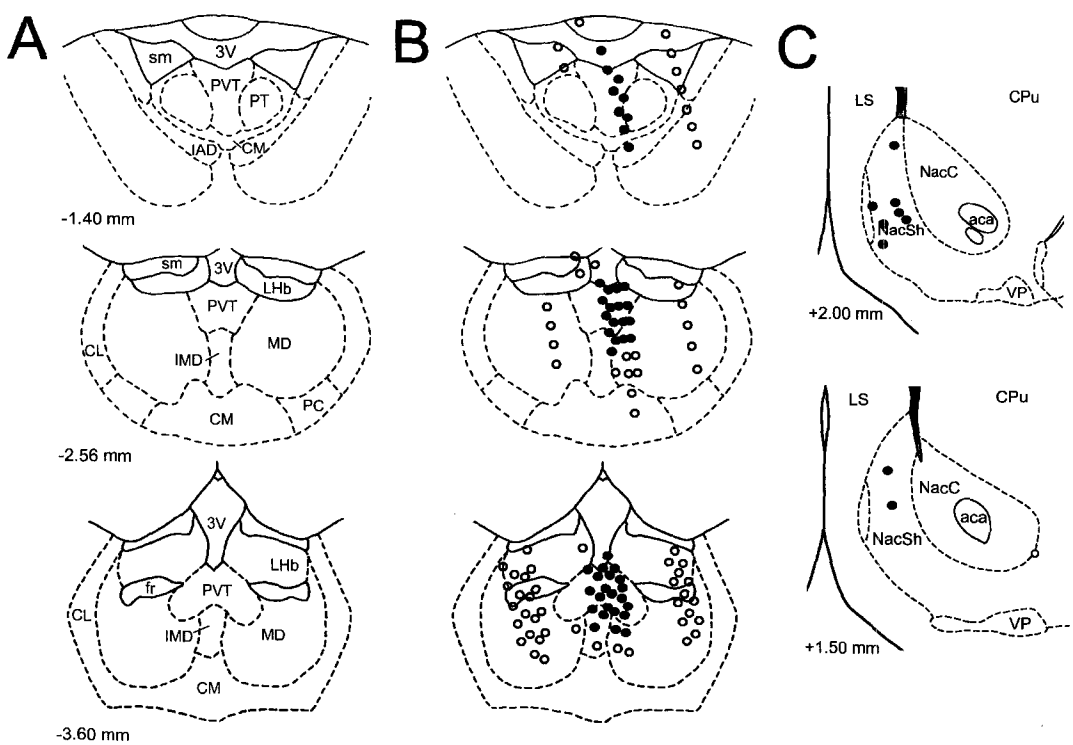
A
B
C
sm
3V
PVT
PT
IAD
CM
-1.40 mm
sm
3V
LHb
PVT
CL
IMD
MD
PC
CM
-2.56 mm
3V
LHb
fr
PVT
CL
IMD
MD
CM
-3.60 mm
LS
CPu
NacC
aca
NacSh
VP
+2.00 mm
LS
CPu
NacC
aca
NacSh
VP
+1.50 mm

in a few cases, but these placements fell in a region directly adjacent to the PVT. The lateral-most portion of the mediodorsal nucleus was stimulated in a number of cases and each time had no effect on oxidation current in the NacSh. Each time a response was found, the current intensity was lowered from 400 μA to determine the lowest stimulation current necessary to elicit an increase in oxidation current within the NacSh. When the stimulating electrode was directly in the PVT responses could be observed using a current intensity of 150μA. No response was ever seen using currents less than 150 μA.

3.4.3 Effect of nomifensine on the PVT-evoked oxidation current in the NacSh

The dopamine uptake inhibitor nomifensine (20 mg/kg; i.p.) was used to confirm the dopaminergic identity of the detected electrochemical event observed in the NacSh following PVT stimulation. By inhibiting dopamine uptake, any PVT-evoked release of dopamine would remain in the extracellular space for a longer period of time and should be reflected in the resulting oxidation current. A PVT-evoked event was compared before and 30 minutes after nomifensine injection. Nomifensine increased the peak (Fig. 14A; $p < 0.05$) as well as the time taken to decay to 80% of the peak value (Fig. 14B; $p < 0.001$) of the oxidation current response. This change was noted as soon as 10 minutes following nomifensine administration and was maintained for at least one hour. Examples of the effect of nomifensine on the response signal are shown from two representative cases (Fig. 14 C, D).

Fig. 14. Effects of nomifensine (20 mg/kg; i.p.) on electrochemical responses in the nucleus accumbens shell (NacSh) evoked by electrical stimulation of the paraventricular nucleus of the thalamus (PVT). Electrical stimulation of the PVT in 5 animals produced a transient increase in NacSh oxidation current detected by constant potential amperometry. Administration of the dopamine uptake inhibitor nomifensine induced a marked increase in the peak of the response evoked by PVT stimulation (A). Nomifensine also increased the time required for a response to diminish 80% from its peak value (T_{80}, B). Examples from two different animals are shown before (*dotted lines*) and after (*solid lines*) nomifensine administration (C, D). Timing of PVT stimulation is presented underneath each response (bar). Data was recorded from 5 animals, and placements of the stimulating and recording electrodes are shown within the PVT and NacSh, respectively (E). Numbers (E) represent approximate distance anterior (+) and posterior (-) to bregma.

*$p < 0.05$; ***$p < 0.001$

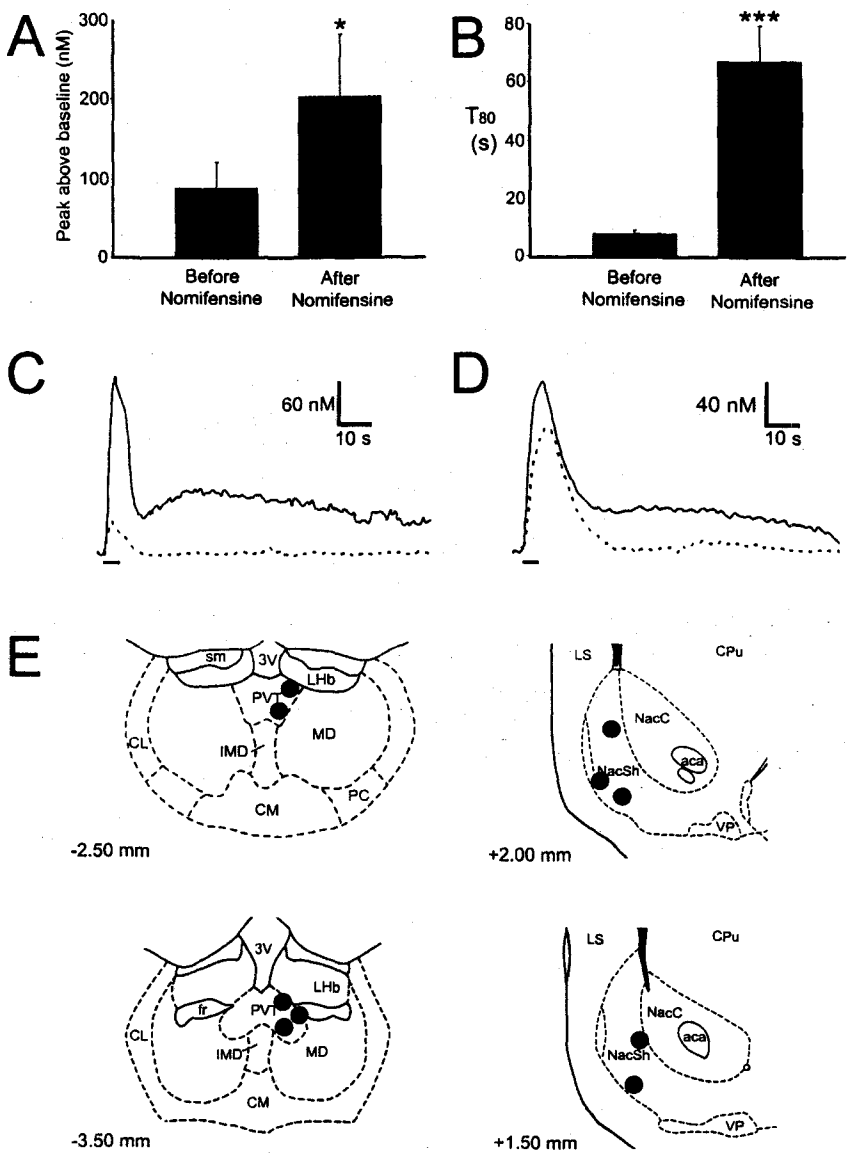
A
Peak above baseline (nM)
300
200
100
0
*
Before Nomifensine
After Nomifensine
B
T80 (s)
80
60
40
20
0
***
Before Nomifensine
After Nomifensine
C
60 nM
10 s
D
40 nM
10 s
E
sm
3V
LHb
PVT
MD
CL
IMD
CM
PC
-2.50 mm
LS
CPu
NacC
aca
NacSh
VP
+2.00 mm
3V
LHb
fr
PVT
CL
IMD
MD
CM
-3.50 mm
LS
CPu
NacC
aca
NacSh
VP
+1.50 mm

3.4.4 Effect of intra-VTA lidocaine on PVT-evoked oxidation current in the NacSh

The effect of large injections of lidocaine in the VTA on PVT-evoked responses was examined to assess the possibility that PVT stimulation produces dopamine efflux via a muti-synaptic excitatory pathway to the VTA. Administration of 2 μl of 4% lidocaine into the VTA induced a decrease in the resting voltammetric signal in the NacSh. This decrease in baseline levels apparent in all 4 animals used for data collection and suggests successful inhibition of dopaminergic activity. The PVT was stimulated at various time points following lidocaine while the oxidation current was monitored in the NacSh. The effect of lidocaine was tested up to one hour following administration and was found to have no effect on the peak and clearance of PVT-evoked oxidation current (Fig. 15 A, B). Tracings showing the evoked signal were strikingly similar before (dotted traces, Fig. 15 C, D) and after lidocaine infusion (solid traces, Fig. 15 C, D). Thus, the PVT-evoked dopamine response in the NacSh does not appear to be mediated by the firing of midbrain dopamine neurons.

3.4.5 Effect of kynurenic acid on PVT-evoked oxidation current in the NacSh

Due to the finding that inhibition of midbrain dopamine neurons had no effect on PVT-evoked dopamine efflux in the NacSh, it is likely that the effect is due to a glutamatergic projection directly from the PVT to the NacSh. To examine the possibility that PVT-evoked dopamine release in the NacSh is dependent upon glutamate release in

Fig. 15. Effects of lidocaine (2 μl, 4%) injections in the ventral tegmental area (VTA) on electrochemical responses in the nucleus accumbens shell (NacSh) evoked by electrical stimulation of the paraventricular nucleus of the thalamus (PVT). Lidocaine infusion into the VTA failed to diminish peak value (A) and clearance rate (B) of the oxidation current in the NacSh evoked by electrical stimulation of the PVT. C, D, Examples from two different animals are shown before (dotted lines) and after (solid lines) lidocaine infusion. Timing of PVT stimulation is presented underneath each response (bar). Data was recorded from 5 animals, and placements of the stimulating and recording electrodes as well as lidocaine infusion sites are shown within the PVT, NacSh, and VTA, respectively (E). Numbers (E) represent approximate distance anterior (+) and posterior (-) to bregma.

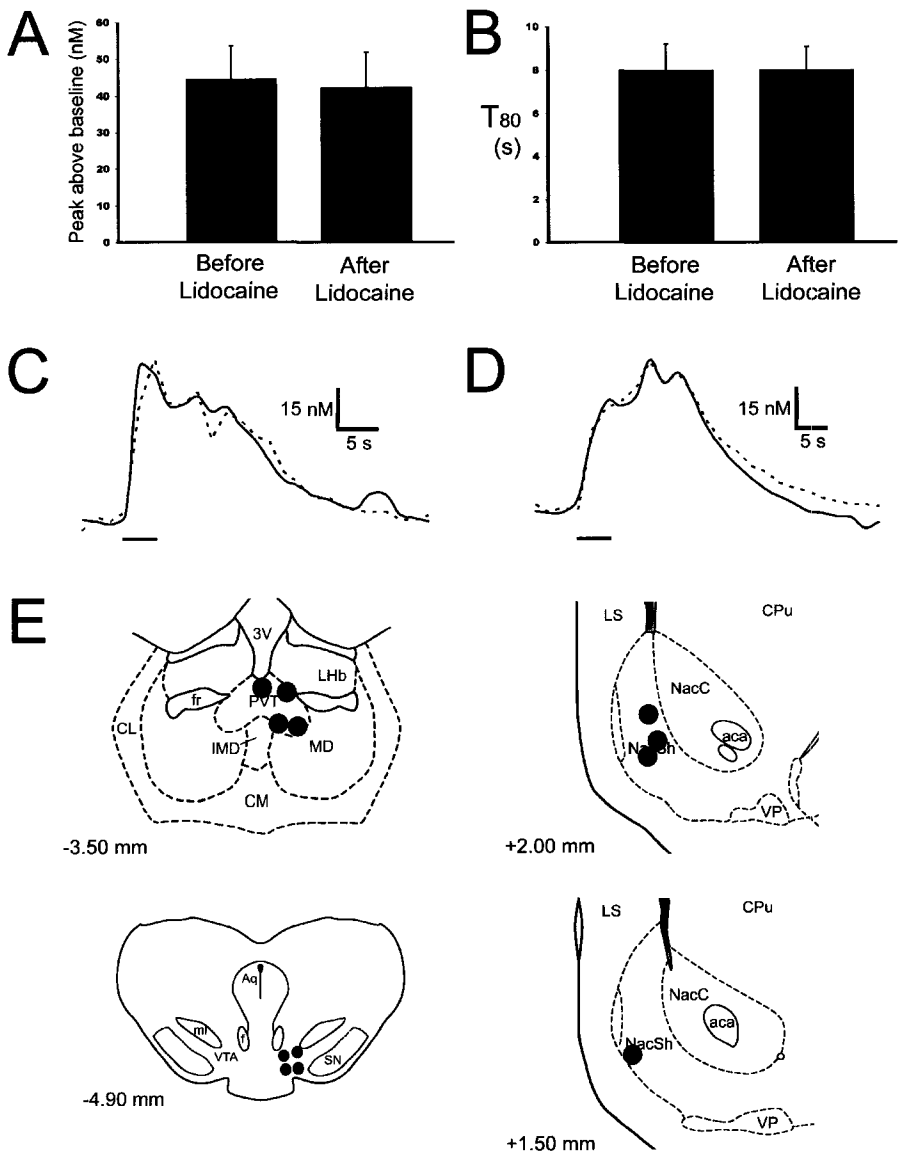
A
Peak above baseline (nM)
Before Lidocaine
After Lidocaine
B
T80 (s)
Before Lidocaine
After Lidocaine
C
15 nM
5 s
D
15 nM
5 s
E
3V
LHb
fr
PVT
CL
IMD
MD
CM
-3.50 mm
LS
CPu
NacC
aca
VP
+2.00 mm
Aq
ml
VTA
SN
-4.90 mm
LS
CPu
NacC
aca
NacSh
VP
+1.50 mm

the NacSh, I examined the effect of blocking ionotropic glutamate receptors in the NacSh using the broad spectrum glutamate receptor antagonist kynurenic acid. The PVT was stimulated before and every 5 minutes after kynurenic acid infusion directly into the NacSh. Kynurenic acid (50 mM, 500 nl) significantly attenuated the size of electrochemical responses in the NacSh following PVT stimulation (Fig. 16; $F_{(5, 35)} = 12.78$; $p < 0.001$). *Post-hoc* comparison (Tukey's) revealed a significant attenuation at the 1, 5, and 10 minute time points tested following kynurenic application.

3.4.6 Effect of apomorphine on PVT-evoked oxidation current in the NacSh

Although kynurenic acid infusion significantly attenuated the PVT-evoked electrochemical response, complete blockade was not observed. To further investigate any involvement of the dopamine neurons in the VTA, the D1/D2 agonist apomorphine was administered (0.15 mg/kg; i.v.) and the PVT was stimulated before and every 5 minutes after apomorphine injection. At this dose, apomorphine completely inhibits dopamine neurons *in vivo* (Grace & Bunney, 1983), a property reflected in the present studies by an observed drop in the resting voltammetric signal following administration. Apomorphine, like lidocaine infusion into the VTA, had no effect on oxidation current evoked by PVT stimulation (Fig. 17).

Fig. 16. Effects of kynurenic acid (KA; 500 nl, 50 mM) on electrochemical responses in the nucleus accumbens shell (NacSh) evoked by electrical stimulation of the paraventricular nucleus of the thalamus (PVT). Kynurenic acid infusion locally within the nucleus accumbens attenuated the magnitude of NacSh oxidation current evoked by PVT stimulation ($p < 0.01$). Responses returned to control values within 30 minutes following KA infusion. Infusion of saline into the NacSh had no effect on PVT-evoked dopamine events in the NacSh.

*$p < 0.05$; **$p < 0.01$

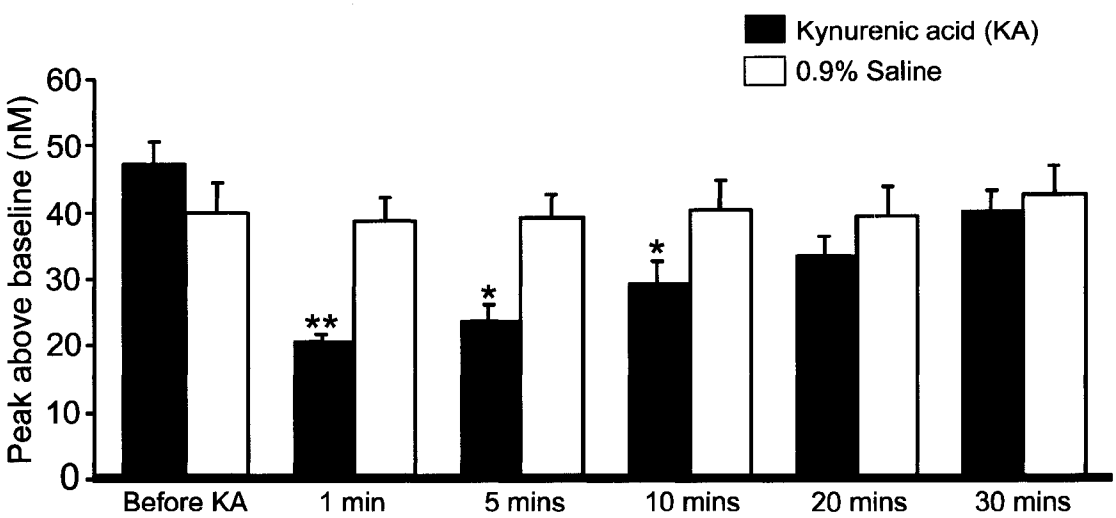
Kynurenic acid (KA)
0.9% Saline
Peak above baseline (nM)
60
50
40
30
20
10
0
**
*
*
Before KA
1 min
5 mins
10 mins
20 mins
30 mins

Fig. 17. Effect of apomorphine (0.15 mg/kg, i.v.) on electrochemical responses in the nucleus accumbens shell (NacSh) evoked by electrical stimulation of the paraventricular nucleus of the thalamus (PVT). Apomorphine did not have any effect on the PVT-evoked oxidation currents observed in the NacSh ($F_{(4, 19)} = 1.31$, $p > 0.05$).

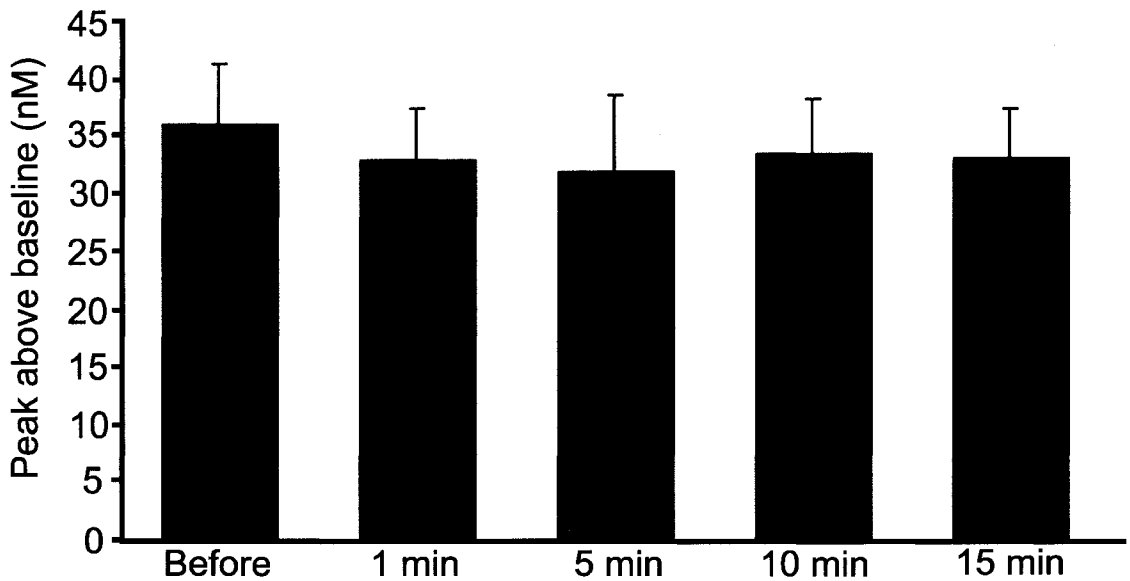
Peak above baseline (nM)
45
40
35
30
25
20
15
10
5
0
Before
1 min
5 min
10 min
15 min

3.4.7 Relationship between anterograde labeling from the PVT and tyrosine hydroxylase immunoreactivity in the NAcSh

Anterograde tracer deposits restricted to the PVT resulted in dense BDA fiber and terminal labeling within the NacSh. Regions of heavy BDA labeling coincided with regions of heavy tyrosine hydroxylase labeling. A representative case is shown where an injection restricted to the right of the midline in the anterior PVT (Fig. 18A) resulted in dense anterograde labeling in the NacSh of the right hemisphere (Fig. 18 B, C).
As previously reported, tyrosine hydroxylase was observed to have a dense heterogeneous distribution within the NacSh compared to the nucleus accumbens core and caudate – putamen. This heterogeneous distribution was matched by fibers anterogradely labeled from the PVT. Examination at high magnification revealed that the dense plexus of BDA fibers overlapped regions of high tyrosine hydroxylase immunoreactivity while avoiding the tyrosine hydroxylase poor areas in the NacSh (Fig. 18 C). Injections of BDA in the anterior PVT resulted in this type of labeling in the dorsomedial and ventromedial shell whereas injections in the posterior PVT produced this pattern in the ventromedial and ventrolateral shell.

Fig. 18. Projections from the paraventricular nucleus of the thalamus (PVT) overlap with tyrosine hydroxylase immunoreactivity within the nucleus accumbens shell (NacSh). Biotin dextran amine (black, BDA) iontophoresis into the PVT (A) resulted in fiber labeling in the NacSh (B, C). Heavy regions of BDA labeling coincide with dense tyrosine hydroxylase activity (brown).

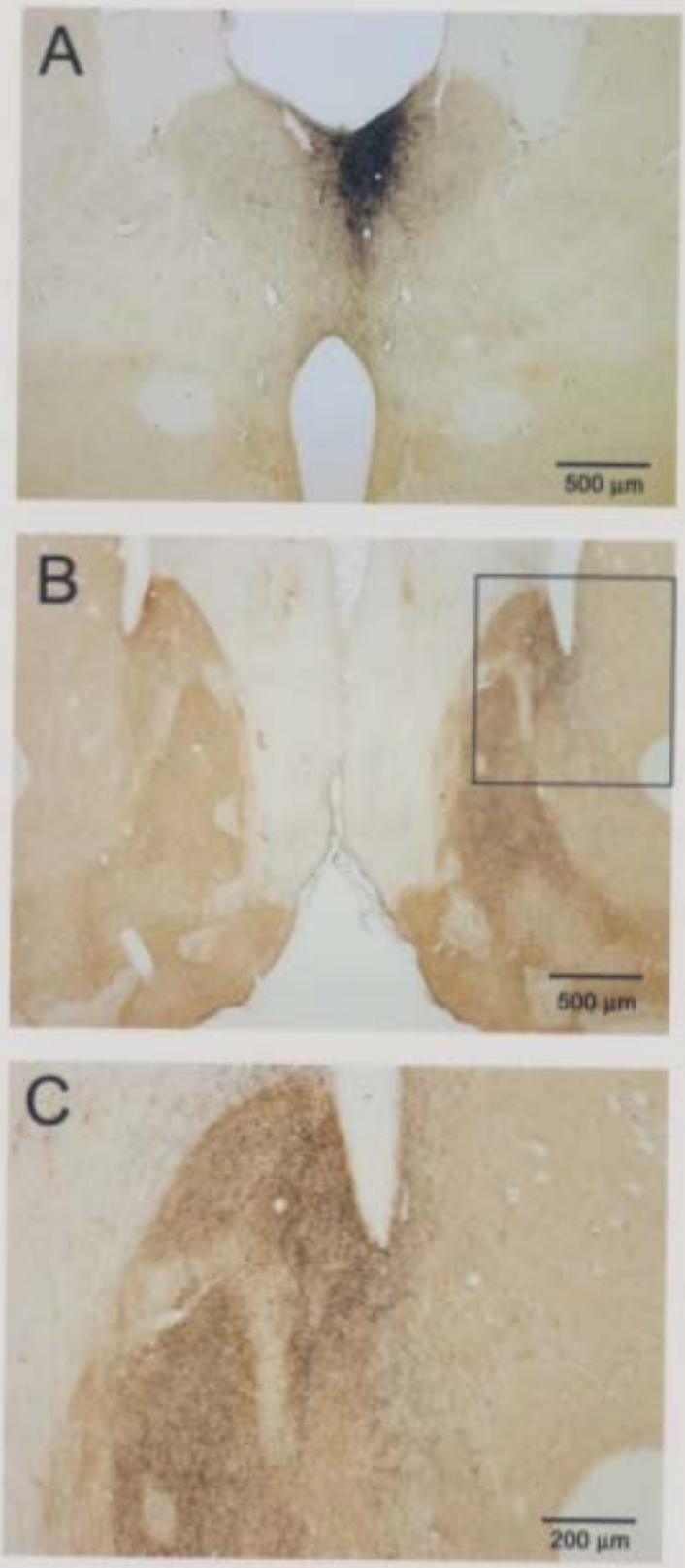
A
500 µm
B
500 µm
C
200 µm

3.4.8 Effect of PVT stimulation on oxidation current throughout the striatum

Oxidation currents were monitored throughout two dorsal-ventral tracts in the striatum while a brief stimulation was applied to the PVT (Fig. 19). PVT-evoked oxidation current increases were noted for every case in which the recording electrode was in the NacSh. Recording sites in the lateral septum located dorsally to the NacSh generated no current change upon PVT stimulation but responses appeared and gradually increased in magnitude as the recording electrode was moved ventrally into the NacSh. For the lateral tract, no response could be seen in the dorsal striatum while a moderate response could be found when the electrode was lowered into the core of the nucleus accumbens. The oxidation currents were monitored in different regions throughout the striatum while the PVT was stimulated at different current intensities. PVT-evoked responses could only be seen in the NacSh when the PVT was stimulated at 150 μA. At this current intensity, no response was seen in the septum, dorsal striatum or nucleus accumbens core. The response in the NacSh could no longer be observed when the PVT was stimulated using currents less than 150 μA.

Fig. 19. The paraventricular nucleus of the thalamus (PVT) was stimulated (400 μA; 1.0 mm pulses at 40 Hz for 5s) while a carbon fiber electrode was adjusted to recorde dopamine oxidation currents in various striatal regions. Stimulation of the PVT increased electrochemically detected dopamine in the nucleus accumbens shell (NacSh) and, to a lesser degree, in the nucleus accumbens core (NacC). PVT stimulation had no effect on oxidation currents dorsal to the NacSh or in the dorsal striatum. Response magnitude was the greatest for placements in the NacSh. aca, anterior commissure; CPu, caudate-putamen.

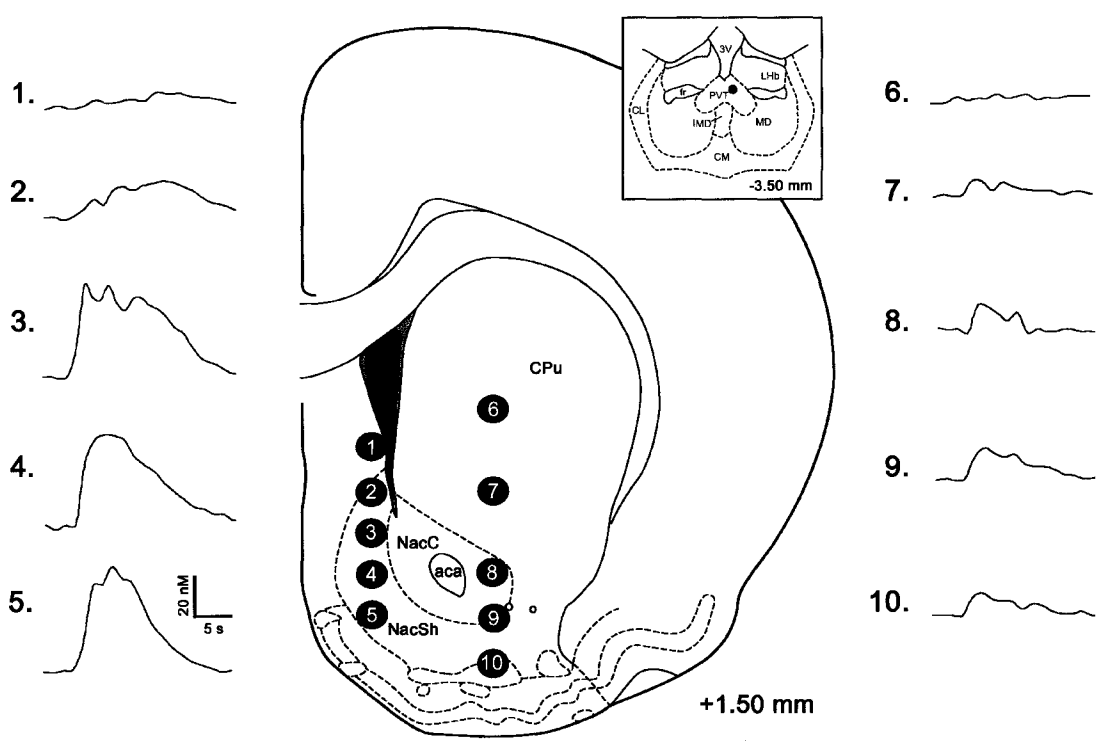
1.
2.
3.
4.
5.
20 nM
5 s
CPu
NacC
aca
NacSh
1
2
3
4
5
6
7
8
9
10
+1.50 mm
3V
LHb
fr
PVT
CL
IMD
MD
CM
-3.50 mm
6.
7.
8.
9.
10.

3.5 Summary

From the results of the present studies, it is suggested that the PVT is unique in that it receives numerous overlapping signals from hypothalamic peptides such as the orexins and CART. Regions of heavy orexin and CART innervation within the midline and intralaminar thalamus coincide with a dense population of PVT neurons projecting to the NacSh. Stimulation of the PVT results in a brief increase in electrochemically-detected dopamine release in the NacSh and is unaffected by the inhibition of midbrain dopamine neurons. However, PVT-evoked dopamine efflux in the NacSh is attenuated following intra-accumbens infusions of the ionotropic glutamate receptor antagonist kynurenic acid, suggesting that the response is mediated by glutamate release from PVT terminals within the NacSh. This is likely to occur via activation of glutamate receptors located on dopamine terminals in the NacSh. The proposed mechanism for a PVT influence on NacSh dopamine release can be seen in Figure 20.

Fig. 20. Schematic diagram demonstrating a likely mechanism by which stimulation of the paraventricular nucleus of the thalamus (PVT) results in a transient increase in dopamine oxidation current within the shell of the nucleus accumbens (NacSh). This proposal suggests that glutamate released from PVT terminals can activate glutamate receptors that are located on dopamine terminals within the NacSh. Although the dopaminergic innervation of the NacSh originates from neurons in the VTA, inhibition of VTA dopamine neurons had no effect upon PVT-evoked dopamine release in the NacSh. Rather, blockade of ionotropic glutamate receptors in the NacSh attenuated the increase in dopamine oxidation current evoked by PVT stimulation. It is suggested that the PVT can presynaptically modulate dopamine release in the NacSh by an impulse-independent mechanism.

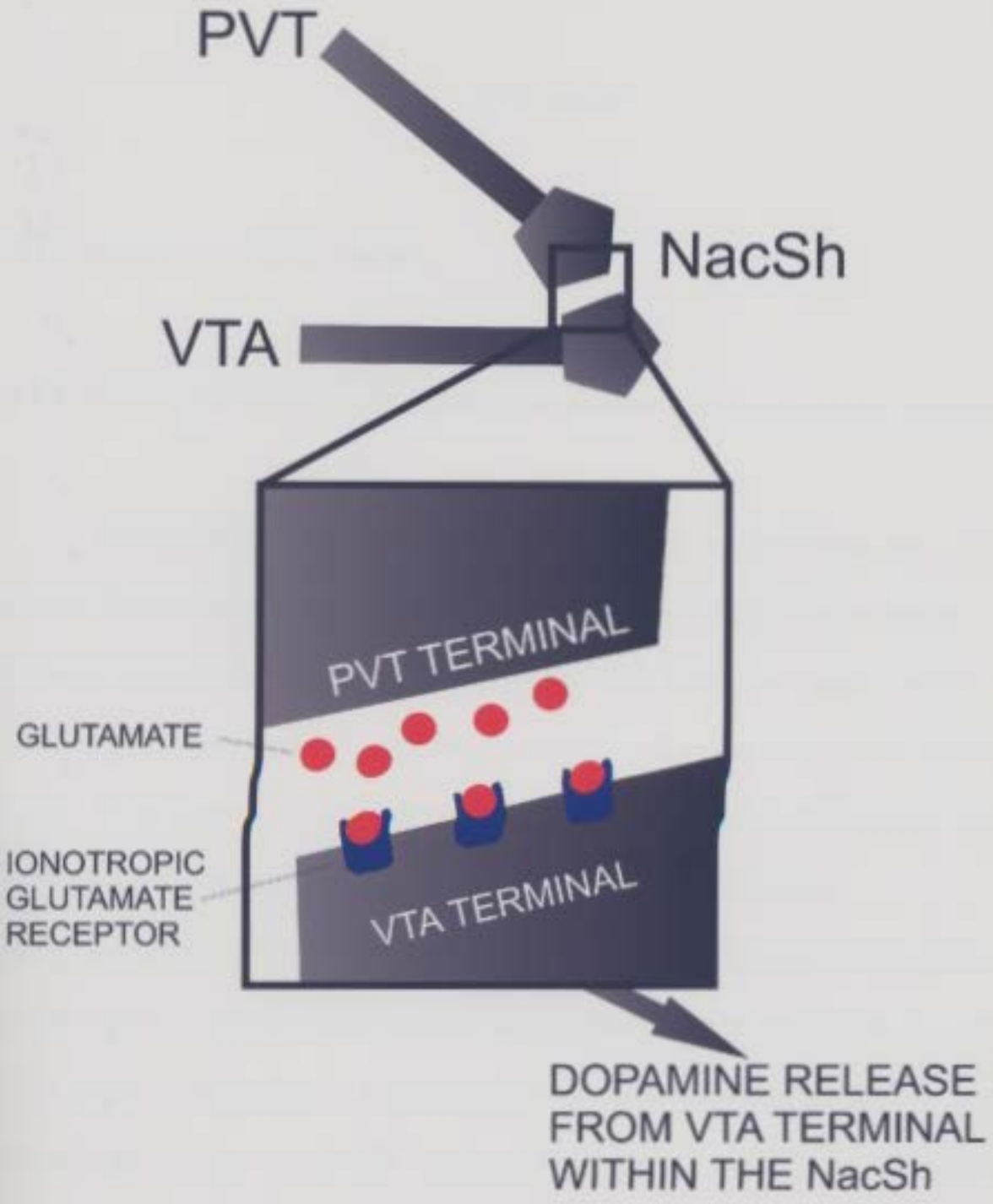
PVT
NacSh
VTA
PVT TERMINAL
GLUTAMATE
IONOTROPIC
GLUTAMATE
RECEPTOR
VTA TERMINAL
DOPAMINE RELEASE
FROM VTA TERMINAL
WITHIN THE NacSh

Chapter 4

Discussion

4.1 Anatomical Experiments

4.1.1. Orexin and CART innervation of the midline and intralaminar thalamus

Immunohistochemistry throughout the PVT revealed that orexin and CART peptide fibers heavily innervate the PVT while adjacent thalamic nuclei receive a relatively weak innervation from these peptides. Both fiber types largely avoided the mediodorsal nucleus and the habenular complex as well as the sensory relay thalamic nuclei. These observations provide the most detailed description of orexin and CART innervation of the midline and intralaminar nuclei to date. Multi-label immunofluorescence with confocal microscopy further revealed that synaptophysin, a marker indicative of presynaptic release, was co-localized on numerous orexin- and CART-positive enlargements. Consistent with these results, a strong signal for orexin receptor mRNA is found in the PVT (Marcus *et al.*, 2001) and PVT neurons are excited by orexin *in vitro* (Ishibashi *et al.*, 2005). However, receptors for the CART peptide have yet to be identified and no study has looked at the effects of CART peptide application on the firing of PVT neurons. While the co-localization of these peptides and synaptophysin

are indicative of release sites, confirmation of these observations at the ultrastructural level are necessary to provide definitive evidence for presynaptic release of orexin and CART in the PVT. Nonetheless, electron microscopy has confirmed that both peptides are packaged in large dense-core vesicles within separate presynaptic sites suggesting that they can be released in the synaptic cleft to influence the postsynaptic neuron (Smith *et al.*, 1999).

4.1.2. Orexin and CART fibers in relation to PVT neurons projecting to the NacSh

Retrograde labeling from the NacSh established that orexin and CART fiber innervation of the PVT heavily overlaps thalamic neurons projecting to the NacSh. High magnification light and confocal imaging techniques provide evidence supporting the existence of orexin and CART fiber contacts onto PVT neurons projecting to the NacSh. Although a large number of neurons in the paratenial nucleus were labeled following tracer injections in the NacSh, this thalamic nucleus contains very weak orexin and CART immunoreactivity. Therefore, the PVT is the only nucleus of the thalamus to receive both orexin and CART afferent input and to project to the NacSh. The retrograde tracer injections into the NacSh varied along its anteroposterior axis to cover the entire NacSh and the resulting retrograde labeling in the thalamus was similar for all ten subjects regardless of whether FG or CTb was used. Labeled neurons were observed in the anterior, middle and posterior PVT, with the most pronounced cluster of retrogradely labeled cells location in more posterior sections.

As mentioned, immunoreactivity for orexin, CART and PVT cells retrogradely labeled from the NacSh was observed throughout the entire PVT. Investigation at high magnification revealed putative contacts between both orexin and CART fibers and PVT neurons projecting to the NacSh throughout the anterior, middle, and posterior PVT. The presence of these contacts did not seem to depend on the anteroposterior placement of the tracer injection within the NacSh. Numerous appositions were observed throughout the 50 μm depth of sections which were stained histochemically with DAB and examined with the light microscope. Although this gives a good understanding of the density of the fiber innervation, light microscopy cannot be used as conclusive evidence for synaptic contact. The confocal microscope was used to provide stronger evidence by ensuring that the observed contacts were within the same plane as the labeled neuron. In fact, numerous appositions could be seen when tissue was scanned at 0.4 μm intervals. It was also demonstrated that a majority of orexin and CART fiber enlargements in the PVT co-express immunoreactivity for the synaptophysin protein. Synaptophysin is a protein involved in presynaptic vesicle release and its frequent co-localization with orexin and CART fiber varicosities indicate that the appositions observed in the present experiments are likely to contain sites of presynaptic release. Although the confocal microscope is a useful tool for the visualization of spatial interactions between fibers and cells of interest, electron microscopy is necessary to fully understand the synaptic nature of these elements. However, confocal imaging proved to be the more suitable choice due to the relative ease of multi-labeling and the ability to sample a larger area of tissue.

Both FG and CTb failed to completely fill PVT neurons. Contacts could only be noted for those immunopositive regions of the cell body and most proximal region of dendrites. Interestingly, more complete cellular staining was evident for retrogradely labeled paratenial cells in anterior thalamic sections. Both CTb and FG tracers are capable of providing complete neuronal staining, a property that unfortunately does not seem to apply to all cell groups. Slight alterations in injection parameters, recovery time, fixation and incubation time did not seem to produce completely stained neurons within the PVT. To overcome this, neurobiotin was infused directly into the PVT to completely fill the soma and proximal dendrites of PVT neurons. Distal dendrites could be seen under the fluorescence microscope but were not able to be picked up by the confocal microscope. In my experience, it seemed that the fluorescence microscope was more sensitive than the confocal microscope. Perhaps this is due to the imaging of the entire section depth combined with a wide wavelength employed to excite the fluorophore of interest. On the other hand, confocal microscopy generates thin optical sections and uses very strict emitted wavelengths to excite the fluorophore and may contribute to the slight sensitivity disadvantage of the confocal microscope. Nonetheless, when combined with orexin or CART immunofluorescence, frequent fiber contact onto the proximal dendrites of PVT neurons could be seen. For the majority of PVT neurons scanned, neuropeptide contacts onto proximal dendrites were just as common as axosomatic appositions. It is concluded that orexin and CART fibers innervate both the soma and proximal dendrites of PVT neurons projecting to the NacSh. Unfortunately, it could not be concluded

whether there are axodendritic contacts on distal dendrites due to the aforementioned problem of labeling distal dendrites.

4.1.3. The PVT as a site of integration of competing signals

An interesting finding is that individual PVT neurons were typically apposed by both the orexin and CART fiber types. The orexins have been shown to frequently co-localize with glutamate, form asymmetric synapses, and have an excitatory effect at the postsynaptic neuron (Ishibashi *et al.*, 2005; Torrealba *et al.*, 2003). Conversely, CART has been shown to frequently co-localize with GABA, form symmetric synapses, and have inhibitory effects at the postsynaptic neuron (Smith *et al.*, 1999; Yermolaieva *et al.*, 2001). The finding that both of these peptide fibers make putative contact onto the same PVT neuron with a known projection to the nucleus accumbens suggests an important role for the PVT in the integration of hypothalamic and brainstem activity. The PVT may act to integrate competing signals from numerous regions and then relay this information to the NacSh. The idea that orexin and CART activity within the PVT would compete to influence PVT neurons activity is supported by research demonstrating an opposite effect of the orexin and CART peptides on food intake. For example, central administration of orexin promotes food intake while CART peptide application inhibits food intake (Sakurai *et al.*, 1998; Vrang *et al.*, 1999). Interestingly, co-application of both orexin and CART was shown to result in feeding behavior identical to that of controls (Volkoff & Peter, 2000). Furthermore, food deprivation up-regulates orexin mRNA and down-

regulates CART mRNA (X. J. Cai *et al.*, 1999; Kristensen *et al.*, 1998). Both orexin and CART neurons co-express immunoreactivity for leptin receptors, and leptin is suggested to have opposite effects on the production and release of the two peptides (Elias *et al.*, 2001; Hakansson *et al.*, 1999; Lopez *et al.*, 2000). Not only does the PVT receive innervation from the orexins and CART, other peptides and monoamines such as alpha-MSH, neuropeptide Y, norepinephrine and serotonin are likely to converge within the PVT and collectively affect the activity of PVT neurons.

4.2. Voltammetry Experiments

The voltammetry experiments show that phasic activation of the PVT produced an increase in oxidation currents recorded in the NacSh. A dopaminergic identity of the evoked oxidation currents is indicated by the property of the nafion-coated carbon fiber electrodes, the observed red/ox ratios and relative concentration of competing molecules within the NacSh, and the changes in electrochemical responses induced by pharmacological manipulation. Electrical stimulation of thalamic nuclei adjacent to the PVT did not produce oxidation currents in the NacSh indicating that the evoked oxidation currents were unique to activation of the PVT. The present study also shows that the transient increases in oxidation currents in the NacSh were attenuated upon intra-accumbens infusion of the general ionotropic glutamate receptor antagonist kynurenic acid but remained unaffected by treatments eliminating the influence of dopamine neuron activity. These results suggest that the PVT can influence dopamine release at the

terminal site and are consistent with a similar mechanism of dopamine modulation reported for other limbic inputs to the NacSh (Blaha *et al.*, 1997; Floresco *et al.*, 1998; Howland *et al.*, 2002).

4.2.1. Electrochemical Specificity

Increases in oxidation current within the NacSh were detected using carbon fiber electrodes which were determined prior to experimentation to have a high selectivity favoring dopamine over ascorbic acid and DOPAC. The negatively-charged nafion coating on each electrode prevented current changes due to the oxidation of these anionic interferents. Selectivity was quantified by adding 2.5 μM of dopamine to a beaker and comparing the response to additions of 250 μM of both ascorbic acid and DOPAC. If necessary, additional nafion coatings were applied until the electrode demonstrated at least a 100:1 selectivity for dopamine over both ascorbic acid and DOPAC. Furthermore, the extracellular concentrations of these interferents are likely to remain at relatively stable levels over short periods of time and are unlikely to be involved in the transient responses measured in our experiments. Another important issue in terms of selectivity is the possibility that changes in norepinephrine and serotonin, two other monoamines that are found in lower concentrations in the NacSh (Allin *et al.*, 1988; Versteeg *et al.*, 1976), could be responsible for the observed oxidation currents following activation of the PVT. Successful chronoamperometric recordings were obtained from a few active sites and a red/ox ratio between 0.7 and 0.8 was observed throughout the duration of PVT-evoked

responses. This red/ox value is indicative of dopamine and not norepinephrine (red/ox = 0.08 – 0.28; Gerhardt & Hoffman, 2001) or serotonin (red/ox = 0.13 – 0.19; Gerhardt & Hoffman, 2001). Discussions on use of chronoamperometry have been published previously (Blaha & Phillips, 1996; Gerhardt & Burmeister, 2000) and this method has been widely used to measure dopamine in the nucleus accumbens. Anatomically, a response was only found upon PVT stimulation when the recording electrode was in a region receiving PVT and tyrosine hydroxylase innervation. Responses could not be observed when the electrode was moved from the NacSh to the adjacent vertical limb of the diagonal band of Broca, a region devoid of tyrosine hydroxylase immunoreactivity. The observation that administration of the dopamine uptake inhibitor nomifensine increased the peak and slowed reuptake of PVT-evoked electrochemical responses in the NacSh is also consistent with the signal representing an evoked dopamine efflux. Together, these data suggest that the increase in oxidation current in the NacSh in response to PVT stimulation represents an increase in dopamine concentration.

4.2.2. Mechanism of PVT-evoked dopamine release in the NacSh

Although the PVT is anatomically positioned to influence dopamine levels via multiple pathways, the present data indicate that the PVT-evoked response is independent of dopamine cell firing. The PVT sends a dense projection to the NacSh and the prefrontal cortex (Bubser & Deutch, 1998; Moga *et al.*, 1995; Otake & Nakamura, 1998; Van der Werf *et al.*, 2002), and both of these regions have direct and indirect projections

to dopamine neurons within the VTA (Geisler & Zahm, 2005; Zahm, 2000; Zahm & Heimer, 1990; Zahm *et al.*, 1996). Infusion of lidocaine into the VTA or systemic administration of apomorphine, two treatments that inactivate dopamine neurons in the midbrain, had no effect on the PVT-evoked responses. This is consistent with studies showing that dopamine release evoked by stimulation of the ventral subiculum of the hippocampus or basolateral nucleus of the amygdala, both of which send a glutamatergic projection to the NacSh, could not be attenuated by inhibiting dopamine cell activity (Blaha *et al.*, 1997; Floresco *et al.*, 1998; Howland *et al.*, 2002). In the present experiments, large decreases in the resting oxidation current were observed in the NacSh following the intra-VTA injections of lidocaine and the systemic injections of apomorphine. This baseline drop is indicative of successful dopamine neuron inhibition and is consistent with previously reported electrochemical reactions to similar treatments (Floresco *et al.*, 1998; Howland *et al.*, 2002). The PVT-evoked oxidation currents in the NacSh remained clearly unaffected by lidocaine and apomorphine indicating that the evoked responses were not mediated by changes in the activity of midbrain dopamine neurons.

Dopamine regulation by limbic afferents to the NacSh has been shown to depend largely on glutamate receptors within the striatum (Blaha *et al.*, 1997; Floresco *et al.*, 1998; Howland *et al.*, 2002). Although dopamine and glutamate terminals have not been observed to form axo-axonic synapses, numerous PVT terminals have been shown to appose dopamine terminals within the NacSh (Pinto *et al.*, 2003). The presence of NMDA receptors on dopamine axons (Gracy & Pickel, 1996) suggests that glutamate

release from PVT terminals can influence dopamine release at the presynaptic level. Reports of the effects of glutamate agonists on local striatal dopamine release are inconsistent; the observed response being dependent on injectate concentration and volume as well as the pipette/electrode tip distance (David *et al.*, 2005; Morari *et al.*, 1998; Whitton, 1997). Despite these inconsistencies, several studies have shown that infusion of high concentrations of NMDA, AMPA, or kainate directly into the striatum can elicit local dopamine release (Carrozza *et al.*, 1992; Keefe *et al.*, 1992, 1993; Martinez-Fong *et al.*, 1992; Sakai *et al.*, 1997; Smolders *et al.*, 1996). In the present study, a significant attenuation of PVT-evoked responses in the NacSh was seen following intra-accumbens infusion of the glutamate receptor antagonist kynurenic acid, suggesting that glutamate release from PVT terminals acts on glutamate receptors within the NacSh to trigger dopamine release. The frequent appositions between PVT and tyrosine hydroxylase fibers as well as the observed attenuation of PVT-evoked oxidation currents following local glutamate receptor antagonism suggests that glutamate release from PVT terminals is involved in the presynaptic regulation of dopamine.

The observed attenuation is believed to result from antagonistic actions at glutamate receptors within the vicinity of the recording electrode. Infusion of both saline and kynurenic acid dissolved in saline resulted in a brief decrease of the voltammetric signal. This baseline drop cannot be attributed to the electrode's response to kynurenic acid itself, as there was no response to kynurenic acid additions *in vitro* during pre-calibration. Furthermore, the drop cannot be attributed to the pharmacological actions of kynurenic acid as the same decrease was observed upon saline administration. This

suggests a dilution of resting dopamine levels near the recording electrode rather than a decrease in dopamine tone itself. Dilution of the analyte as a result of local drug administration has been previously reported (Blaha *et al.*, 1997; Floresco *et al.*, 1998; Blaha & Phillips; 1996) and intra-striatal infusions of kynurenic acid has been shown to have no effect on dopamine levels (Keefe *et al.*, 1993). There were a few cases in which this decrease was not apparent, and were later shown histologically to be due to a distance greater than 600 μm between the tips of the infusion pipette and recording electrode. A lateral distance of approximately 500 μm has been reported to be the limit of neuronal inactivation following GABA injection into the visual cortex (Hupe *et al.*, 1999). According to this, injection volumes used in the present study would not be able to overcome a large separation between the pipette and electrode tips. Therefore, if a baseline drop is not observed upon local drug infusion, it is likely that the volume did not reach the immediate area of the recording electrode and cannot exert its pharmacological actions at that site. Not surprisingly, if a baseline drop was not apparent in the present study, the treatment seemed to have no effect on the properties of PVT-evoked responses. These cases were subsequently dropped from data analysis. PVT-evoked responses were attenuated in all subjects responding initially to kynurenic acid infusion with a small decrease in baseline. Although the same baseline drop was observed upon saline infusion, saline alone had no effect on PVT-evoked dopamine responses.

The precise mechanism by which glutamate release from PVT terminals in the NacSh might regulate dopamine release locally remains to be determined. First, the release of glutamate by phasic activation of the PVT may depolarize dopamine terminals

by acting on ionotropic receptors located on the dopamine fiber resulting in Ca++ influx and release of dopamine. Second, cholinergic nicotinic receptors found on dopamine fibers in the striatum (I. W. Jones *et al.*, 2001) have been shown to regulate striatal dopamine release (Fu *et al.*, 2000; Fung, 1989; Zhou *et al.*, 2001). PVT fibers have been shown to innervate cholinergic interneurons in the NacSh (Meredith & Wouterlood, 1990) and provides another mechanism by which glutamate afferents to the NacSh may regulate local dopamine release. Third, a recent *in vivo* experiment provides evidence for glutamate to act locally on ionotropic receptors in the striatum to maintain tonic levels of dopamine by a reverse transport mechanism mediated by the dopamine transporter (Borland & Michael, 2004). In this case, dopamine release would occur via activation of reverse transport of dopamine and not from release from synaptic vesicles (Leviel, 2001). However, PVT-evoked dopamine release in the NacSh in the present experiments is not likely due to a reverse transport mechanism because systemic administration of the dopamine uptake inhibitor nomifensine did not attenuate the PVT evoked responses. Nonetheless, the exact mechanism by which glutamate release from PVT terminals elicits dopamine release in the NacSh remains to be determined.

4.2.3. Differential regulation of dopamine release in the heterogeneous NacSh

The conclusion that PVT stimulation evokes dopamine efflux in the NacSh is further supported by the relationship observed between the recording electrode placements in the striatum and the magnitude of the response recorded from stimulation

of the PVT. Stimulation of the PVT produced the largest oxidation currents when the recording electrode was placed in the NacSh. Consistent with previous anterograde and retrograde tract tracing studies (Berendse & Groenewegen, 1990; Moga *et al.*, 1995; Su & Bentivoglio, 1990), I found that the PVT sends a dense projection to the NacSh and a moderate projection to the core of the nucleus accumbens. Therefore, it is especially striking that stimulation of the PVT evoked the largest oxidation current responses in the NacSh whereas only moderate responses could be elicited in the core. The PVT does not provide input to the rest of the dorsal striatum and no oxidation current responses were observed in the dorsal striatum upon PVT stimulation. However, other midline and intralaminar thalamic nuclei provide inputs to different subregions of the striatum (Groenewegen & Berendse, 1994). Even though I did not examine the effects of stimulation of adjacent thalamic nuclei, it is possible that these areas of the thalamus can modulate dopamine levels in regions of the dorsal striatum.

The present data demonstrate that the tyrosine hydroxylase staining has a heterogeneous distribution in the NacSh and that the PVT preferentially innervates the regions of dense staining. This is consistent with other anterograde studies showing that the PVT projections to the NacSh targets areas moderately stained for enkephalin (Berendse & Groenewegen, 1990), the same areas which receive a dense dopaminergic innervation (Voorn *et al.*, 1986). Although PVT stimulation typically resulted in an oxidation current increase in the NacSh corresponding to dopamine levels in the magnitude of 40 – 50 nM, a few cases were observed in which these transients peaked upwards of 200 nM. Therefore, it is possible that sites that gave the largest responses

may have resulted from voltammetry recordings in regions receiving a very dense dopamine and PVT fiber innevation. It is also of interest that the regions of the NacSh containing dense dopamine and PVT inputs correspond to the same regions that receive afferents from the ventral subiculum (Groenewegen *et al.*, 1987). Areas of the NacSh with weak dopamine immunoreactivity and avoided by PVT afferents receive inputs from the basolateral nucleus of the amygdala and the medial prefrontal cortex (Wright & Groenewegen, 1995). Each of these sub-territories appears to have unique set of dopamine receptors, neurotransmitters and projection targets (Heimer *et al.*, 1997). Consequently, differential regulation of dopamine release within these sub-regions by specific glutamatergic inputs may have different physiological functions. The extent and significance of differential regulation of dopamine release within sub-territories of the NacSh may be helpful in providing a better understanding of the role of dopamine in the NacSh.

4.2.4 Dopamine release and NacSh output

The consequence of increased dopamine efflux within the NacSh is difficult to interpret, given the interactions between dopamine itself and glutamatergic afferents from the prefrontal cortex, amygdala and hippocampus. Nonetheless, dopamine application to nucleus accumbens slices has been shown to increase spike frequency in medium spiny neurons and this effect is dependent upon activation of both D1 and D2-like receptors (Hopf *et al.*, 2003). Furthermore, dopamine was found to decrease glutamate release

through activation of D2-like receptors located presynaptically whereas infusions of D1 receptor antagonists had no effect on glutamate release within the accumbens (Maura et *al.*, 1988; Yamamoto & Davy, 1992). It is likely that the PVT-evoked dopamine release observed in the present studies may affect behavioral output by increasing the activity of medium spiny output neurons of the NacSh via co-activation of D1 and D2 receptors on the postsynaptic neuron as well as through presynaptic inhibition of glutamate release.

4.3. Significance

The anatomical data provide evidence that orexin and CART neuropeptides can influence the nucleus accumbens using the PVT as a site of integration and relay. Although the current work concerns orexin and CART fibers in the PVT, several other neuropeptides have been reported to heavily innervate the PVT (Freedman & Cassell, 1994; Otake & Nakamura, 1995). This places the PVT in an anatomical position to receive convergent information from hypothalamic neuropeptides and brainstem monoamines and then integrate and relay this activity to the nucleus accumbens, an area of the striatum involved in motivational responding and behavioral activation.

The voltammetry experiments demonstrate that the PVT plays a role in the modulation of tonic dopamine tone in the NacSh. In addition to the PVT, the NacSh receives glutamatergic inputs from the ventral subiculum of the hippocampus, basaolateral nucleus of the amygdala and medial prefrontal cortex. These convergent glutamate afferents have been shown to influence dopamine release in the NacSh (Blaha

et al., 1997; Floresco *et al.*, 1998; Howland *et al.*, 2002) and interaction between these inputs is likely to play an important role in overall dopamine regulation and therefore the selection and initiation of behavioral activity (Groenewegen *et al.*, 1987; Mogenson *et al.*, 1980; Mogenson & Yang, 1991). The PVT, by receiving afferents from hypothalamic peptides such as orexin and CART as well as from numerous brainstem arousal nuclei (Freedman & Cassell, 1994; Kirouac *et al.*, 2005; Otake, 2005; Otake *et al.*, 2002; Otake & Ruggiero, 1995; Van der Werf *et al.*, 2002), is highly responsive to stress and arousal (Bubser & Deutch, 1999; Otake *et al.*, 2002; Peng *et al.*, 1995). Interestingly, dopamine levels in the nucleus accumbens peak during periods of active waking (Castaneda *et al.*, 2004; Lena *et al.*, 2005) and increase dramatically during periods associated with stress (Kalivas & Duffy, 1995; Stevenson *et al.*, 2003). A similar pattern of activity is observed in the PVT in that expression of c-fos mRNA and c-Fos protein is enhanced during periods of active waking and greatly increased following exposure to a stress protocol (Bubser & Deutch, 1999; Otake *et al.*, 2002; Sica *et al.*, 2000; Timofeeva & Richard, 2001). This is the first report demonstrating an influence of the PVT on tonic dopamine levels in the striatum. While speculative at this point, arousal related activation of the PVT may be important for motivation through an arousal-based maintenance or stress-induced increase of tonic dopamine levels in the NacSh (Blackburn *et al.*, 1992; Horvitz, 2000; Salamone & Correa, 2002).

Overall, the present thesis demonstrates that orexin and CART peptide fibers appose PVT neurons projecting to the NacSh and that PVT stimulation can influence levels of extrasynaptic dopamine release within the NacSh. Although the PVT receives a

wide variety of arousal-related afferent inputs, numerous peptides projecting to the PVT are involved in food intake. It can be proposed that this hypothalamic-thalamic-striatal projection functions in part to regulate motivated behavior related to feeding. As mentioned in section 1.3, intracerebroventricular application of the orexin and CART neuropeptides dramatically influence food intake, and food deprivation or overfeeding regulates the expression of mRNA encoding these peptides. The PVT is also heavily innervated by other hypothalamic peptides involved in energy homeostasis such as neuropeptide Y, cholecystokinin, agouti related peptide and alpha-MSH (Freedman & Cassell, 1994). The present thesis also demonstrates that the same PVT neuron is frequently innervated by both orexin and CART peptide fibers. The heavy innervation of the PVT by other hypothalamic peptides raises the possibility that a given PVT neuron is innervated by a number of signals representing energy balance. It is not surprising that PVT lesions influence both food intake and anticipatory reactions to an expected food reward (Bhatnagar & Dallman, 1999; Nakahara *et al.*, 2004). By demonstrating that the PVT has a glutamate-dependant presynaptic influence on tonic dopamine levels in the NacSh, it is likely that energy homeostatic signals represented in the PVT are transmitted to the NacSh where dopamine levels are altered accordingly to initiate an appropriate behavioral response. A number of studies suggest that dopamine levels in the NacSh are not implicated in the reward value of a food reward, rather demonstrating a dopaminergic role in the initiation of a consummatory response. Salamone (Salamone *et al.*, 2003) argues that nucleus accumbens dopamine is critical to the initiation of energy expenditure to obtain food reward in an instrumental learning paradigm, a theory consistent with the

association between the NacSh and motivation. In agreement, others have raised the notion that accumbens dopamine is not involved in the primary reinforcing properties of food reward ("liking") but rather in aspects of incentive salience ("wanting"). This is well observed in studies using a choice test in which rats can either lever press for a preferred food reward or simply consume, without any lever pressing, a less desirable food. A variety of dopamine antagonists, administered either systemically or locally within the accumbens, has been shown to substantially reduce the probability that an animal will exert effort to obtain the preferred reward (Koch *et al.*, 2000; Salamone & Correa, 2002). Further support for an accumbens/dopamine role in the initiation of feeding arises from voltammetric recordings of behaving animals. By monitoring dopamine oxidation currents within the NacSh on a subsecond timescale, Roitman *et al.*, (2004) demonstrated that when a salient cue was paired with subsequent food reward, dopamine efflux was observed immediately following the cue and prior to the presentation and receipt of the reward. These data suggest that tonic dopamine increases within the NacSh play a role in food-seeking behavior and is consistent with a hypothalamic-thalamic-striatal circuit involved in initiating appropriate behavioral responses to homeostatic challenge.

References

Allin, R., Russell, V. A., Lamm, M. C., & Taljaard, J. J. (1988). Regional distribution of monoamines in the nucleus accumbens of the rat. *Neurochem Res, 13*(10), 937-942.

Antonelli, T., Govoni, B. M., Bianchi, C., & Beani, L. (1997). Glutamate regulation of dopamine release in guinea pig striatal slices. *Neurochem Int, 30*(2), 203-209.

Balkan, B., Koylu, E., Pogun, S., & Kuhar, M. J. (2003). Effects of adrenalectomy on cart expression in the rat arcuate nucleus. *Synapse, 50*(1), 14-19.

Balkan, B., Koylu, E. O., Kuhar, M. J., & Pogun, S. (2001). The effect of adrenalectomy on cocaine and amphetamine-regulated transcript (cart) expression in the hypothalamic nuclei of the rat. *Brain Res, 917*(1), 15-20.

Bassareo, V., & Di Chiara, G. (1999). Modulation of feeding-induced activation of mesolimbic dopamine transmission by appetitive stimuli and its relation to motivational state. *Eur J Neurosci, 11*(12), 4389-4397.

Berendse, H. W., & Groenewegen, H. J. (1990). Organization of the thalamostriatal projections in the rat, with special emphasis on the ventral striatum. *J Comp Neurol, 299*(2), 187-228.

Berendse, H. W., & Groenewegen, H. J. (1991). Restricted cortical termination fields of the midline and intralaminar thalamic nuclei in the rat. *Neuroscience, 42*(1), 73-102.

Beuckmann, C. T., Sinton, C. M., Williams, S. C., Richardson, J. A., Hammer, R. E., Sakurai, T., *et al.* (2004). Expression of a poly-glutamine-ataxin-3 transgene in

orexin neurons induces narcolepsy-cataplexy in the rat. *J Neurosci, 24*(18), 4469-4477.

Beuckmann, C. T., & Yanagisawa, M. (2002). Orexins: From neuropeptides to energy homeostasis and sleep/wake regulation. *J Mol Med, 80*(6), 329-342.

Bhatnagar, S., & Dallman, M. (1998). Neuroanatomical basis for facilitation of hypothalamic-pituitary-adrenal responses to a novel stressor after chronic stress. *Neuroscience, 84*(4), 1025-1039.

Bhatnagar, S., & Dallman, M. F. (1999). The paraventricular nucleus of the thalamus alters rhythms in core temperature and energy balance in a state-dependent manner. *Brain Res, 851*(1-2), 66-75.

Blackburn, J. R., Pfaus, J. G., & Phillips, A. G. (1992). Dopamine functions in appetitive and defensive behaviours. *Prog Neurobiol, 39*(3), 247-279.

Blaha, C. D., & Phillips, A. G. (1996). A critical assessment of electrochemical procedures applied to the measurement of dopamine and its metabolites during drug-induced and species-typical behaviours. *Behav Pharmacol, 7*(7), 675-708.

Blaha, C. D., Yang, C. R., Floresco, S. B., Barr, A. M., & Phillips, A. G. (1997). Stimulation of the ventral subiculum of the hippocampus evokes glutamate receptor-mediated changes in dopamine efflux in the rat nucleus accumbens. *Eur J Neurosci, 9*(5), 902-911.

Borland, L. M., & Michael, A. C. (2004). Voltammetric study of the control of striatal dopamine release by glutamate. *J Neurochem, 91*(1), 220-229.

Bowyer, J. F., Scallet, A. C., Holson, R. R., Lipe, G. W., Slikker, W., Jr., & Ali, S. F. (1991). Interactions of mk-801 with glutamate-, glutamine- and methamphetamine-evoked release of [3h]dopamine from striatal slices. *J Pharmacol Exp Ther, 257*(1), 262-270.

Bubser, M., & Deutch, A. Y. (1998). Thalamic paraventricular nucleus neurons collateralize to innervate the prefrontal cortex and nucleus accumbens. *Brain Res, 787*(2), 304-310.

Bubser, M., & Deutch, A. Y. (1999). Stress induces fos expression in neurons of the thalamic paraventricular nucleus that innervate limbic forebrain sites. *Synapse, 32*(1), 13-22.

Cai, N. S., Kiss, B., & Erdo, S. L. (1991). Heterogeneity of n-methyl-d-aspartate receptors regulating the release of dopamine and acetylcholine from striatal slices. *J Neurochem, 57*(6), 2148-2151.

Cai, X. J., Widdowson, P. S., Harrold, J., Wilson, S., Buckingham, R. E., Arch, J. R., *et al.* (1999). Hypothalamic orexin expression: Modulation by blood glucose and feeding. *Diabetes, 48*(11), 2132-2137.

Carrozza, D. P., Ferraro, T. N., Golden, G. T., Reyes, P. F., & Hare, T. A. (1992). In vivo modulation of excitatory amino acid receptors: Microdialysis studies on n-methyl-d-aspartate-evoked striatal dopamine release and effects of antagonists. *Brain Res, 574*(1-2), 42-48.

Castaneda, T. R., de Prado, B. M., Prieto, D., & Mora, F. (2004). Circadian rhythms of dopamine, glutamate and gaba in the striatum and nucleus accumbens of the awake rat: Modulation by light. *J Pineal Res, 36*(3), 177-185.

Charara, A., & Grace, A. A. (2003). Dopamine receptor subtypes selectively modulate excitatory afferents from the hippocampus and amygdala to rat nucleus accumbens neurons. *Neuropsychopharmacology, 28*(8), 1412-1421.

Chemelli, R. M., Willie, J. T., Sinton, C. M., Elmquist, J. K., Scammell, T., Lee, C., *et al.* (1999). Narcolepsy in orexin knockout mice: Molecular genetics of sleep regulation. *Cell, 98*(4), 437-451.

Chen, S., & Su, H. S. (1990). Afferent connections of the thalamic paraventricular and parataenial nuclei in the rat--a retrograde tracing study with iontophoretic application of fluoro-gold. *Brain Res, 522*(1), 1-6.

Clow, D. W., & Jhamandas, K. (1989). Characterization of l-glutamate action on the release of endogenous dopamine from the rat caudate-putamen. *J Pharmacol Exp Ther, 248*(2), 722-728.

Cornwall, J., & Phillipson, O. T. (1988). Afferent projections to the dorsal thalamus of the rat as shown by retrograde lectin transport. Ii. The midline nuclei. *Brain Res Bull, 21*(2), 147-161.

Cutler, D. J., Morris, R., Sheridhar, V., Wattam, T. A., Holmes, S., Patel, S., *et al.* (1999). Differential distribution of orexin-a and orexin-b immunoreactivity in the rat brain and spinal cord. *Peptides, 20*(12), 1455-1470.

D'Angio, M., Serrano, A., Rivy, J. P., & Scatton, B. (1987). Tail-pinch stress increases extracellular dopac levels (as measured by in vivo voltammetry) in the rat nucleus accumbens but not frontal cortex: Antagonism by diazepam and zolpidem. *Brain Res, 409*(1), 169-174.

Date, Y., Ueta, Y., Yamashita, H., Yamaguchi, H., Matsukura, S., Kangawa, K., *et al.* (1999). Orexins, orexigenic hypothalamic peptides, interact with autonomic, neuroendocrine and neuroregulatory systems. *Proc Natl Acad Sci U S A, 96*(2), 748-753.

David, H. N., Ansseau, M., & Abraini, J. H. (2005). Dopamine-glutamate reciprocal modulation of release and motor responses in the rat caudate-putamen and nucleus accumbens of "intact" animals. *Brain Res Brain Res Rev, 50*(2), 336-360.

de Lecea, L., Kilduff, T. S., Peyron, C., Gao, X., Foye, P. E., Danielson, P. E., *et al.* (1998). The hypocretins: Hypothalamus-specific peptides with neuroexcitatory activity. *Proc Natl Acad Sci U S A, 95*(1), 322-327.

de Lecea, L., Sutcliffe, J. G., & Fabre, V. (2002). Hypocretins/orexins as integrators of physiological information: Lessons from mutant animals. *Neuropeptides, 36*(2-3), 85-95.

Deutch, A. Y., & Cameron, D. S. (1992). Pharmacological characterization of dopamine systems in the nucleus accumbens core and shell. *Neuroscience, 46*(1), 49-56.

Doherty, M. D., & Gratton, A. (1992). High-speed chronoamperometric measurements of mesolimbic and nigrostriatal dopamine release associated with repeated daily stress. *Brain Res, 586*(2), 295-302.

Dominguez, G., Vicentic, A., Del Giudice, E. M., Jaworski, J., Hunter, R. G., & Kuhar, M. J. (2004). Cart peptides: Modulators of mesolimbic dopamine, feeding, and stress. *Ann N Y Acad Sci, 1025*, 363-369.

Douglass, J., McKinzie, A. A., & Couceyro, P. (1995). Pcr differential display identifies a rat brain mrna that is transcriptionally regulated by cocaine and amphetamine. *J Neurosci, 15*(3 Pt 2), 2471-2481.

Dube, M. G., Kalra, S. P., & Kalra, P. S. (1999). Food intake elicited by central administration of orexins/hypocretins: Identification of hypothalamic sites of action. *Brain Res, 842*(2), 473-477.

Elias, C. F., Lee, C. E., Kelly, J. F., Ahima, R. S., Kuhar, M., Saper, C. B., *et al.* (2001). Characterization of cart neurons in the rat and human hypothalamus. *J Comp Neurol, 432*(1), 1-19.

Espana, R. A., Valentino, R. J., & Berridge, C. W. (2003). Fos immunoreactivity in hypocretin-synthesizing and hypocretin-1 receptor-expressing neurons: Effects of diurnal and nocturnal spontaneous waking, stress and hypocretin-1 administration. *Neuroscience, 121*(1), 201-217.

Ferguson, A. V., & Samson, W. K. (2003). The orexin/hypocretin system: A critical regulator of neuroendocrine and autonomic function. *Front Neuroendocrinol, 24*(3), 141-150.

Floresco, S. B., Yang, C. R., Phillips, A. G., & Blaha, C. D. (1998). Basolateral amygdala stimulation evokes glutamate receptor-dependent dopamine efflux in the nucleus accumbens of the anaesthetized rat. *Eur J Neurosci, 10*(4), 1241-1251.

Freedman, L. J., & Cassell, M. D. (1994). Relationship of thalamic basal forebrain projection neurons to the peptidergic innervation of the midline thalamus. *J Comp Neurol, 348*(3), 321-342.

Fu, Y., Matta, S. G., Gao, W., & Sharp, B. M. (2000). Local alpha-bungarotoxin-sensitive nicotinic receptors in the nucleus accumbens modulate nicotine-stimulated dopamine secretion in vivo. *Neuroscience, 101*(2), 369-375.

Fung, Y. K. (1989). Effects of chronic nicotine pretreatment on (+)-amphetamine and nicotine-induced synthesis and release of [3h]dopamine from [3h]tyrosine in rat nucleus accumbens. *J Pharm Pharmacol, 41*(1), 66-68.

Gambarana, C., Masi, F., Tagliamonte, A., Scheggi, S., Ghiglieri, O., & De Montis, M. G. (1999). A chronic stress that impairs reactivity in rats also decreases dopaminergic transmission in the nucleus accumbens: A microdialysis study. *J Neurochem, 72*(5), 2039-2046.

Geisler, S., & Zahm, D. S. (2005). Afferents of the ventral tegmental area in the rat-anatomical substratum for integrative functions. *J Comp Neurol, 490*(3), 270-294.

Gerashchenko, D., Kohls, M. D., Greco, M., Waleh, N. S., Salin-Pascual, R., Kilduff, T. S., *et al.* (2001). Hypocretin-2-saporin lesions of the lateral hypothalamus produce narcoleptic-like sleep behavior in the rat. *J Neurosci, 21*(18), 7273-7283.

Gerhardt, G. A., & Burmeister, J. J. (2000). In vivo voltammetry for chemical analysis of the nervous system. *J. Encyclopedia of Analytical Chemistry.*

Gerhardt, G. A., & Hoffman, A. F. (2001). Effects of recording media composition on the responses of nafion-coated carbon fiber microelectrodes measured using high-speed chronoamperometry. *J Neurosci Methods, 109*(1), 13-21.

Grace, A. A. (1991). Phasic versus tonic dopamine release and the modulation of dopamine system responsivity: A hypothesis for the etiology of schizophrenia. *Neuroscience, 41*(1), 1-24.

Grace, A. A. (2000). Gating of information flow within the limbic system and the pathophysiology of schizophrenia. *Brain Res Brain Res Rev, 31*(2-3), 330-341.

Grace, A. A., & Bunney, B. S. (1983). Intracellular and extracellular electrophysiology of nigral dopaminergic neurons--1. Identification and characterization. *Neuroscience, 10*(2), 301-315.

Gracy, K. N., & Pickel, V. M. (1996). Ultrastructural immunocytochemical localization of the n-methyl-d-aspartate receptor and tyrosine hydroxylase in the shell of the rat nucleus accumbens. *Brain Res, 739*(1-2), 169-181.

Groenewegen, H. J., & Berendse, H. W. (1994). The specificity of the 'nonspecific' midline and intralaminar thalamic nuclei. *Trends Neurosci, 17*(2), 52-57.

Groenewegen, H. J., Vermeulen-Van der Zee, E., te Kortschot, A., & Witter, M. P. (1987). Organization of the projections from the subiculum to the ventral striatum in the rat. A study using anterograde transport of phaseolus vulgaris leucoagglutinin. *Neuroscience, 23*(1), 103-120.

Hagan, J. J., Leslie, R. A., Patel, S., Evans, M. L., Wattam, T. A., Holmes, S., *et al.* (1999). Orexin a activates locus coeruleus cell firing and increases arousal in the rat. *Proc Natl Acad Sci U S A, 96*(19), 10911-10916.

Hakansson, M., de Lecea, L., Sutcliffe, J. G., Yanagisawa, M., & Meister, B. (1999). Leptin receptor- and stat3-immunoreactivities in hypocretin/orexin neurones of the lateral hypothalamus. *J Neuroendocrinol, 11*(8), 653-663.

Hara, J., Beuckmann, C. T., Nambu, T., Willie, J. T., Chemelli, R. M., Sinton, C. M., *et al.* (2001). Genetic ablation of orexin neurons in mice results in narcolepsy, hypophagia, and obesity. *Neuron, 30*(2), 345-354.

Heimer, L., Alheid, G. F., de Olmos, J. S., Groenewegen, H. J., Haber, S. N., Harlan, R. E., *et al.* (1997). The accumbens: Beyond the core-shell dichotomy. *J Neuropsychiatry Clin Neurosci, 9*(3), 354-381.

Hopf, F. W., Cascini, M. G., Gordon, A. S., Diamond, I., Bonci, A. (2003). Cooperative activation of dopamine D1 and D2 receptors increases spike firing of nucleus accumbens neurons via G-protein betagamma subunits. *J. Neurosci, 23(12),* 5079-87

Horvitz, J. C. (2000). Mesolimbocortical and nigrostriatal dopamine responses to salient non-reward events. *Neuroscience, 96*(4), 651-656.

Howland, J. G., Taepavarapruk, P., & Phillips, A. G. (2002). Glutamate receptor-dependent modulation of dopamine efflux in the nucleus accumbens by basolateral, but not central, nucleus of the amygdala in rats. *J Neurosci, 22*(3), 1137-1145.

Hunter, R. G., Philpot, K., Vicentic, A., Dominguez, G., Hubert, G. W., & Kuhar, M. J. (2004). Cart in feeding and obesity. *Trends Endocrinol Metab, 15*(9), 454-459.

Hupe, J. M., Chouvet, G., & Bullier, J. (1999). Spatial and temporal parameters of cortical inactivation by gaba. *J Neurosci Methods, 86*(2), 129-143.

Iravani, M. M., & Kruk, Z. L. (1996). Real-time effects of n-methyl-d-aspartic acid on dopamine release in slices of rat caudate putamen: A study using fast cyclic voltammetry. *J Neurochem, 66*(3), 1076-1085.

Ishibashi, M., Takano, S., Yanagida, H., Takatsuna, M., Nakajima, K., Oomura, Y., *et al.* (2005). Effects of orexins/hypocretins on neuronal activity in the paraventricular nucleus of the thalamus in rats in vitro. *Peptides, 26*(3), 471-481.

Johnson, K. M., & Jeng, Y. J. (1991). Pharmacological evidence for n-methyl-d-aspartate receptors on nigrostriatal dopaminergic nerve terminals. *Can J Physiol Pharmacol, 69*(10), 1416-1421.

Jones, B. E., & Yang, T. Z. (1985). The efferent projections from the reticular formation and the locus coeruleus studied by anterograde and retrograde axonal transport in the rat. *J Comp Neurol, 242*(1), 56-92.

Jones, I. W., Bolam, J. P., & Wonnacott, S. (2001). Presynaptic localisation of the nicotinic acetylcholine receptor beta2 subunit immunoreactivity in rat nigrostriatal dopaminergic neurones. *J Comp Neurol, 439*(2), 235-247.

Kalivas, P. W., & Duffy, P. (1995). Selective activation of dopamine transmission in the shell of the nucleus accumbens by stress. *Brain Res, 675*(1-2), 325-328.

Keefe, K. A., Zigmond, M. J., & Abercrombie, E. D. (1992). Extracellular dopamine in striatum: Influence of nerve impulse activity in medial forebrain bundle and local glutamatergic input. *Neuroscience, 47*(2), 325-332.

Keefe, K. A., Zigmond, M. J., & Abercrombie, E. D. (1993). In vivo regulation of extracellular dopamine in the neostriatum: Influence of impulse activity and local excitatory amino acids. *J Neural Transm Gen Sect, 91*(2-3), 223-240.

Kirouac, G. J., Parsons, M. P., & Li, S. (2005). Orexin (hypocretin) innervation of the paraventricular nucleus of the thalamus. *Brain Res, 1059*(2), 179-188.

Koch, M., Schmid, A., & Schnitzler, H. U. (2000). Role of muscles accumbens dopamine d1 and d2 receptors in instrumental and pavlovian paradigms of conditioned reward. *Psychopharmacology (Berl), 152*(1), 67-73.

Kodama, T., Usui, S., Honda, Y., & Kimura, M. (2005). High fos expression during the active phase in orexin neurons of a diurnal rodent, tamias sibiricus barberi. *Peptides, 26*(4), 631-638.

Koylu, E. O., Couceyro, P. R., Lambert, P. D., & Kuhar, M. J. (1998). Cocaine- and amphetamine-regulated transcript peptide immunohistochemical localization in the rat brain. *J Comp Neurol, 391*(1), 115-132.

Koylu, E. O., Couceyro, P. R., Lambert, P. D., Ling, N. C., DeSouza, E. B., & Kuhar, M. J. (1997). Immunohistochemical localization of novel cart peptides in rat hypothalamus, pituitary and adrenal gland. *J Neuroendocrinol, 9*(11), 823-833.

Krebs, M. O., Desce, J. M., Kemel, M. L., Gauchy, C., Godeheu, G., Cheramy, A., *et al.* (1991). Glutamatergic control of dopamine release in the rat striatum: Evidence

for presynaptic n-methyl-d-aspartate receptors on dopaminergic nerve terminals. *J Neurochem, 56*(1), 81-85.

Kristensen, P., Judge, M. E., Thim, L., Ribel, U., Christjansen, K. N., Wulff, B. S., *et al.* (1998). Hypothalamic cart is a new anorectic peptide regulated by leptin. *Nature, 393*(6680), 72-76.

Krout, K. E., Belzer, R. E., & Loewy, A. D. (2002). Brainstem projections to midline and intralaminar thalamic nuclei of the rat. *J Comp Neurol, 448*(1), 53-101.

Krout, K. E., & Loewy, A. D. (2000a). Parabrachial nucleus projections to midline and intralaminar thalamic nuclei of the rat. *J Comp Neurol, 428*(3), 475-494.

Krout, K. E., & Loewy, A. D. (2000b). Periaqueductal gray matter projections to midline and intralaminar thalamic nuclei of the rat. *J Comp Neurol, 424*(1), 111-141.

Kukkonen, J. P., Holmqvist, T., Ammoun, S., & Akerman, K. E. (2002). Functions of the orexinergic/hypocretinergic system. *Am J Physiol Cell Physiol, 283*(6), C1567-1591.

Kulagina, N. V., Zigmond, M. J., & Michael, A. C. (2001). Glutamate regulates the spontaneous and evoked release of dopamine in the rat striatum. *Neuroscience, 102*(1), 121-128.

Lambert, P. D., Couceyro, P. R., McGirr, K. M., Dall Vechia, S. E., Smith, Y., & Kuhar, M. J. (1998). Cart peptides in the central control of feeding and interactions with neuropeptide y. *Synapse, 29*(4), 293-298.

Lena, I., Parrot, S., Deschaux, O., Muffat-Joly, S., Sauvinet, V., Renaud, B., *et al.* (2005). Variations in extracellular levels of dopamine, noradrenaline, glutamate, and

aspartate across the sleep--wake cycle in the medial prefrontal cortex and nucleus accumbens of freely moving rats. *J Neurosci Res, 81*(6), 891-899.

Leviel, V. (2001). The reverse transport of da, what physiological significance? *Neurochem Int, 38*(2), 83-106.

Li, H. Y., Hwang, H. W., & Hu, Y. H. (2002). Functional characterizations of cocaine- and amphetamine-regulated transcript mrna expression in rat hypothalamus. *Neurosci Lett, 323*(3), 203-206.

Lopez, M., Seoane, L., Garcia, M. C., Lago, F., Casanueva, F. F., Senaris, R., *et al.* (2000). Leptin regulation of prepro-orexin and orexin receptor mrna levels in the hypothalamus. *Biochem Biophys Res Commun, 269*(1), 41-45.

Maldonado-Irizarry, C. S., Swanson, C. J., & Kelley, A. E. (1995). Glutamate receptors in the nucleus accumbens shell control feeding behavior via the lateral hypothalamus. *J Neurosci, 15*(10), 6779-6788.

Marcus, J. N., Aschkenasi, C. J., Lee, C. E., Chemelli, R. M., Saper, C. B., Yanagisawa, M., *et al.* (2001). Differential expression of orexin receptors 1 and 2 in the rat brain. *J Comp Neurol, 435*(1), 6-25.

Martinez-Fong, D., Rosales, M. G., Gongora-Alfaro, J. L., Hernandez, S., & Aceves, J. (1992). Nmda receptor mediates dopamine release in the striatum of unanesthetized rats as measured by brain microdialysis. *Brain Res, 595*(2), 309-315.

Matthysse, S. (1973). Antipsychotic drug actions: A clue to the neuropathology of schizophrenia? *Fed Proc, 32*(2), 200-205.

Maura, G., Giardi, A., Raiteri, M. (1988). Release-regulating D-2 dopamine receptors are located on striatal glutamatergic nerve terminals. *J Phamacol Exp Ther. 247*, 680-684.

Meredith, G. E., & Wouterlood, F. G. (1990). Hippocampal and midline thalamic fibers and terminals in relation to the choline acetyltransferase-immunoreactive neurons in nucleus accumbens of the rat: A light and electron microscopic study. *J Comp Neurol, 296*(2), 204-221.

Moga, M. M., Weis, R. P., & Moore, R. Y. (1995). Efferent projections of the paraventricular thalamic nucleus in the rat. *J Comp Neurol, 359*(2), 221-238.

Mogenson, G. J., Jones, D. L., & Yim, C. Y. (1980). From motivation to action: Functional interface between the limbic system and the motor system. *Prog Neurobiol, 14*(2-3), 69-97.

Mogenson, G. J., & Yang, C. R. (1991). The contribution of basal forebrain to limbic-motor integration and the mediation of motivation to action. *Adv Exp Med Biol, 295*, 267-290.

Morari, M., Marti, M., Sbrenna, S., Fuxe, K., Bianchi, C., & Beani, L. (1998). Reciprocal dopamine-glutamate modulation of release in the basal ganglia. *Neurochem Int, 33*(5), 383-397.

Nakahara, K., Fukui, K., & Murakami, N. (2004). Involvement of thalamic paraventricular nucleus in the anticipatory reaction under food restriction in the rat. *J Vet Med Sci, 66*(10), 1297-1300.

Nambu, T., Sakurai, T., Mizukami, K., Hosoya, Y., Yanagisawa, M., & Goto, K. (1999). Distribution of orexin neurons in the adult rat brain. *Brain Res, 827*(1-2), 243-260.

Nishino, S., Fujiki, N., Ripley, B., Sakurai, E., Kato, M., Watanabe, T., *et al.* (2001). Decreased brain histamine content in hypocretin/orexin receptor-2 mutated narcoleptic dogs. *Neurosci Lett, 313*(3), 125-128.

Nishino, S., Ripley, B., Overeem, S., Lammers, G. J., & Mignot, E. (2000). Hypocretin (orexin) deficiency in human narcolepsy. *Lancet, 355*(9197), 39-40.

Novak, C. M., Harris, J. A., Smale, L., & Nunez, A. A. (2000a). Suprachiasmatic nucleus projections to the paraventricular thalamic nucleus in nocturnal rats (rattus norvegicus) and diurnal nile grass rats (arviacanthis niloticus). *Brain Res, 874*(2), 147-157.

Novak, C. M., & Nunez, A. A. (1998). Daily rhythms in fos activity in the rat ventrolateral preoptic area and midline thalamic nuclei. *Am J Physiol, 275*(5 Pt 2), R1620-1626.

Novak, C. M., Smale, L., & Nunez, A. A. (2000b). Rhythms in fos expression in brain areas related to the sleep-wake cycle in the diurnal arvicanthis niloticus. *Am J Physiol Regul Integr Comp Physiol, 278*(5), R1267-1274.

Otake, K. (2005). Cholecystokinin and substance p immunoreactive projections to the paraventricular thalamic nucleus in the rat. *Neurosci Res, 51*(4), 383-394.

Otake, K., Kin, K., & Nakamura, Y. (2002). Fos expression in afferents to the rat midline thalamus following immobilization stress. *Neurosci Res, 43*(3), 269-282.

Otake, K., & Nakamura, Y. (1995). Sites of origin of corticotropin-releasing factor-like immunoreactive projection fibers to the paraventricular thalamic nucleus in the rat. *Neurosci Lett, 201*(1), 84-86.

Otake, K., & Nakamura, Y. (1998). Single midline thalamic neurons projecting to both the ventral striatum and the prefrontal cortex in the rat. *Neuroscience, 86*(2), 635-649.

Otake, K., & Ruggiero, D. A. (1995). Monoamines and nitric oxide are employed by afferents engaged in midline thalamic regulation. *J Neurosci, 15*(3 Pt 1), 1891-1911.

Parsons, M. P., Li, S., & Kirouac, G. J. (2006). The paraventricular nucleus of the thalamus as an interface between the orexin and cart peptides and the shell of the nucleus accumbens. *Synapse, 59*(8), 480-490.

Paxinos, G., & Watson, C. (2005). The rat brain in stereotaxic coordinates: The new coronal set. *5*.

Peng, Z. C., Grassi-Zucconi, G., & Bentivoglio, M. (1995). Fos-related protein expression in the midline paraventricular nucleus of the rat thalamus: Basal oscillation and relationship with limbic efferents. *Exp Brain Res, 104*(1), 21-29.

Peyron, C., Tighe, D. K., van den Pol, A. N., de Lecea, L., Heller, H. C., Sutcliffe, J. G., *et al.* (1998). Neurons containing hypocretin (orexin) project to multiple neuronal systems. *J Neurosci, 18*(23), 9996-10015.

Pinto, A., Jankowski, M., & Sesack, S. R. (2003). Projections from the paraventricular nucleus of the thalamus to the rat prefrontal cortex and nucleus accumbens shell:

Ultrastructural characteristics and spatial relationships with dopamine afferents. *J Comp Neurol, 459*(2), 142-155.

Ragnauth, A., Znamensky, V., Moroz, M., & Bodnar, R. J. (2000). Analysis of dopamine receptor antagonism upon feeding elicited by mu and delta opioid agonists in the shell region of the nucleus accumbens. *Brain Res, 877*(1), 65-72.

Ramsey, J. J., Kemnitz, J. W., Newton, W., Hagopian, K., Patterson, T. A., & Swick, A. G. (2005). Food intake in rhesus monkeys following central administration of orexins. *Regul Pept, 124*(1-3), 209-214.

Rodgers, R. J., Ishii, Y., Halford, J. C., & Blundell, J. E. (2002). Orexins and appetite regulation. *Neuropeptides, 36*(5), 303-325.

Rohner-Jeanrenaud, F., Craft, L. S., Bridwell, J., Suter, T. M., Tinsley, F. C., Smiley, D. L., *et al.* (2002). Chronic central infusion of cocaine- and amphetamine-regulated transcript (cart 55-102): Effects on body weight homeostasis in lean and high-fat-fed obese rats. *Int J Obes Relat Metab Disord, 26*(2), 143-149.

Roitman, M. F., Stuber, G. D., Phillips, P. E., Wightman, R. M., & Carelli, R. M. (2004). Dopamine operates as a subsecond modulator of food seeking. *J Neurosci, 24*(6), 1265-1271.

Royce, G. J., Bromley, S., Gracco, C., & Beckstead, R. M. (1989). Thalamocortical connections of the rostral intralaminar nuclei: An autoradiographic analysis in the cat. *J Comp Neurol, 288*(4), 555-582.

Ruggiero, D. A., Anwar, S., Kim, J., & Glickstein, S. B. (1998). Visceral afferent pathways to the thalamus and olfactory tubercle: Behavioral implications. *Brain Res, 799*(1), 159-171.

Sakai, K., Akiyama, K., Kashihara, K., Tsuchida, K., Ujike, H., Kuroda, S., *et al.* (1997). Ampa receptors modulate dopamine release in the striatum, as measured by brain microdialysis. *Neurochem Int, 30*(3), 329-336.

Sakurai, T., Amemiya, A., Ishii, M., Matsuzaki, I., Chemelli, R. M., Tanaka, H., *et al.* (1998). Orexins and orexin receptors: A family of hypothalamic neuropeptides and g protein-coupled receptors that regulate feeding behavior. *Cell, 92*(4), 573-585.

Salamone, J. D., & Correa, M. (2002). Motivational views of reinforcement: Implications for understanding the behavioral functions of nucleus accumbens dopamine. *Behav Brain Res, 137*(1-2), 3-25.

Salamone, J. D., Correa, M., Mingote, S., & Weber, S. M. (2003). Nucleus accumbens dopamine and the regulation of effort in food-seeking behavior: Implications for studies of natural motivation, psychiatry, and drug abuse. *J Pharmacol Exp Ther, 305*(1), 1-8.

Salamone, J. D., Correa, M., Mingote, S. M., & Weber, S. M. (2005). Beyond the reward hypothesis: Alternative functions of nucleus accumbens dopamine. *Curr Opin Pharmacol, 5*(1), 34-41.

Savontaus, E., Conwell, I. M., & Wardlaw, S. L. (2002). Effects of adrenalectomy on agrp, pomc, npy and cart gene expression in the basal hypothalamus of fed and fasted rats. *Brain Res, 958*(1), 130-138.

Sica, A. L., Greenberg, H. E., Scharf, S. M., & Ruggiero, D. A. (2000). Chronic-intermittent hypoxia induces immediate early gene expression in the midline thalamus and epithalamus. *Brain Res, 883*(2), 224-228.

Siegel, J. M. (2004). Hypocretin (orexin): Role in normal behavior and neuropathology. *Annu Rev Psychol, 55*, 125-148.

Smith, Y., Kieval, J., Couceyro, P. R., & Kuhar, M. J. (1999). Cart peptide-immunoreactive neurones in the nucleus accumbens in monkeys: Ultrastructural analysis, colocalization studies, and synaptic interactions with dopaminergic afferents. *J Comp Neurol, 407*(4), 491-511.

Smolders, I., Sarre, S., Vanhaesendonck, C., Ebinger, G., & Michotte, Y. (1996). Extracellular striatal dopamine and glutamate after decortication and kainate receptor stimulation, as measured by microdialysis. *J Neurochem, 66*(6), 2373-2380.

Spiess, J., Villarreal, J., & Vale, W. (1981). Isolation and sequence analysis of a somatostatin-like polypeptide from ovine hypothalamus. *Biochemistry, 20*(7), 1982-1988.

Stevens, J. R. (1973). An anatomy of schizophrenia? *Arch Gen Psychiatry, 29*(2), 177-189.

Stevenson, C. W., Sullivan, R. M., & Gratton, A. (2003). Effects of basolateral amygdala dopamine depletion on the nucleus accumbens and medial prefrontal cortical dopamine responses to stress. *Neuroscience, 116*(1), 285-293.

Stone, T. W. (1993). Neuropharmacology of quinolinic and kynurenic acids. *Pharmacol Rev, 45*(3), 309-379.

Su, H. S., & Bentivoglio, M. (1990). Thalamic midline cell populations projecting to the nucleus accumbens, amygdala, and hippocampus in the rat. *J Comp Neurol, 297*(4), 582-593.

Swanson, C. J., Heath, S., Stratford, T. R., & Kelley, A. E. (1997). Differential behavioral responses to dopaminergic stimulation of nucleus accumbens subregions in the rat. *Pharmacol Biochem Behav, 58*(4), 933-945.

Sweet, D. C., Levine, A. S., Billington, C. J., & Kotz, C. M. (1999). Feeding response to central orexins. *Brain Res, 821*(2), 535-538.

Tachibana, T., Takagi, T., Tomonaga, S., Ohgushi, A., Ando, R., Denbow, D. M., *et al.* (2003). Central administration of cocaine- and amphetamine-regulated transcript inhibits food intake in chicks. *Neurosci Lett, 337*(3), 131-134.

Taheri, S., Zeitzer, J. M., & Mignot, E. (2002). The role of hypocretins (orexins) in sleep regulation and narcolepsy. *Annu Rev Neurosci, 25*, 283-313.

Thannickal, T. C., Moore, R. Y., Nienhuis, R., Ramanathan, L., Gulyani, S., Aldrich, M., *et al.* (2000). Reduced number of hypocretin neurons in human narcolepsy. *Neuron, 27*(3), 469-474.

Timofeeva, E., & Richard, D. (2001). Activation of the central nervous system in obese zucker rats during food deprivation. *J Comp Neurol, 441*(1), 71-89.

Torrealba, F., Yanagisawa, M., & Saper, C. B. (2003). Colocalization of orexin a and glutamate immunoreactivity in axon terminals in the tuberomammillary nucleus in rats. *Neuroscience, 119*(4), 1033-1044.

Van der Werf, Y. D., Witter, M. P., & Groenewegen, H. J. (2002). The intralaminar and midline nuclei of the thalamus. Anatomical and functional evidence for participation in processes of arousal and awareness. *Brain Res Brain Res Rev, 39*(2-3), 107-140.

Versteeg, D. H., Van Der Gugten, J., De Jong, W., & Palkovits, M. (1976). Regional concentrations of noradrenaline and dopamine in rat brain. *Brain Res, 113*(3), 563-574.

Volkoff, H., & Peter, R. E. (2000). Effects of cart peptides on food consumption, feeding and associated behaviors in the goldfish, carassius auratus: Actions on neuropeptide y- and orexin a-induced feeding. *Brain Res, 887*(1), 125-133.

Voorn, P., Jorritsma-Byham, B., Van Dijk, C., & Buijs, R. M. (1986). The dopaminergic innervation of the ventral striatum in the rat: A light- and electron-microscopical study with antibodies against dopamine. *J Comp Neurol, 251*(1), 84-99.

Vrang, N., Larsen, P. J., Tang-Christensen, M., Larsen, L. K., & Kristensen, P. (2003). Hypothalamic cocaine-amphetamine regulated transcript (cart) is regulated by glucocorticoids. *Brain Res, 965*(1-2), 45-50.

Vrang, N., Tang-Christensen, M., Larsen, P. J., & Kristensen, P. (1999). Recombinant cart peptide induces c-fos expression in central areas involved in control of feeding behaviour. *Brain Res, 818*(2), 499-509.

Wang, J. K. (1991). Presynaptic glutamate receptors modulate dopamine release from striatal synaptosomes. *J Neurochem, 57*(3), 819-822.

Whitton, P. S. (1997). Glutamatergic control over brain dopamine release in vivo and in vitro. *Neurosci Biobehav Rev, 21*(4), 481-488.

Willie, J. T., Chemelli, R. M., Sinton, C. M., Tokita, S., Williams, S. C., Kisanuki, Y. Y., *et al.* (2003). Distinct narcolepsy syndromes in orexin receptor-2 and orexin null mice: Molecular genetic dissection of non-rem and rem sleep regulatory processes. *Neuron, 38*(5), 715-730.

Willie, J. T., Chemelli, R. M., Sinton, C. M., & Yanagisawa, M. (2001). To eat or to sleep? Orexin in the regulation of feeding and wakefulness. *Annu Rev Neurosci, 24*, 429-458.

Wright, C. I., & Groenewegen, H. J. (1995). Patterns of convergence and segregation in the medial nucleus accumbens of the rat: Relationships of prefrontal cortical, midline thalamic, and basal amygdaloid afferents. *J Comp Neurol, 361*(3), 383-403.

Yamamoto, B. K., & Davy, S. (1992). Dopaminergic modulation of glutamate release in striatum as measured by microdialysis. *J Neurochem, 58,* 1736-1742

Yermolaieva, O., Chen, J., Couceyro, P. R., & Hoshi, T. (2001). Cocaine- and amphetamine-regulated transcript peptide modulation of voltage-gated ca2+ signaling in hippocampal neurons. *J Neurosci, 21*(19), 7474-7480.

Yoshida, Y., Fujiki, N., Nakajima, T., Ripley, B., Matsumura, H., Yoneda, H., *et al.* (2001). Fluctuation of extracellular hypocretin-1 (orexin a) levels in the rat in relation to the light-dark cycle and sleep-wake activities. *Eur J Neurosci, 14*(7), 1075-1081.

Zahm, D. S. (1992). Subsets of neurotensin-immunoreactive neurons revealed following antagonism of the dopamine-mediated suppression of neurotensin immunoreactivity in the rat striatum. *Neuroscience, 46*(2), 335-350.

Zahm, D. S. (2000). An integrative neuroanatomical perspective on some subcortical substrates of adaptive responding with emphasis on the nucleus accumbens. *Neurosci Biobehav Rev, 24*(1), 85-105.

Zahm, D. S., & Heimer, L. (1990). Two transpallidal pathways originating in the rat nucleus accumbens. *J Comp Neurol, 302*(3), 437-446.

Zahm, D. S., Williams, E., & Wohltmann, C. (1996). Ventral striatopallidothalamic projection: Iv. Relative involvements of neurochemically distinct subterritories in the ventral pallidum and adjacent parts of the rostroventral forebrain. *J Comp Neurol, 364*(2), 340-362.

Zhou, F. M., Liang, Y., & Dani, J. A. (2001). Endogenous nicotinic cholinergic activity regulates dopamine release in the striatum. *Nat Neurosci, 4*(12), 1224-1229.